UTRECHT UNIVERSITY

KONINKLIJK NEDERLANDS METEOROLOGISCH INSTITUUT

INSTITUTE FOR MARINE AND ATMOSPHERIC RESEARCH UTRECHT

Climate Physics MSc Thesis

Ocean surface wind properties of different scatterometer observation types and numerical weather prediction model fields

Project supervisor: **Michiel Baatsen**

KNMI supervision: **Rianne Giesen** and **Ad Stoffelen**

Second examiner: **Claudia Wieners**

Jorge Miguel Fernández

Student number: 2008890

June 2023

Abstract:

Understanding surface wind divergence is crucial for multiple physical mechanisms such as convection and pressure adjustments. During the entire year 2022 five scatterometer instruments on MetOp-B, MetOp-C, HY-2B, HY-2C and HY-2D satellites were operational at the same time. Taking advantage of this opportunity, this thesis conducts an analysis of the differences in surface wind divergence between observations from the available satellites and the operational IFS model of ECMWF. In addition, comparison between observations of different scatterometers are performed. The analyses focus on the North Atlantic and the Tropical Atlantic regions, where two important phenomena for the surface wind divergence can be found: the Gulf Stream and the ITCZ.

Overall, ASCAT observations show more variability and a higher proportion of extreme wind divergence values in comparison with HSCAT. This is particularly noticeable in the ITCZ and Gulf Stream regions, where convergence extremes are more prevalent.

These study's findings indicate that the operational ECMWF model exhibits a greater bias in wind divergence when compared to the ASCAT satellites (MetOp-B and MetOp-C) than with HSCAT satellites (HY-2B, HY-2C and HY-2D). Particularly, on the Tropical Atlantic, significant bias is found on the ITCZ area with ASCAT and HSCAT instruments for the winter and summer months of 2022.

Furthermore, the results reveal more consistency between MetOp-B and MetOp-C observations over the Tropical Atlantic than over the North Atlantic. However, the model biases perceived by ASCAT and HSCAT satellites is greater over the Tropical Atlantic than over the North Atlantic. In consequence, it demonstrates that the operational ECMWF model presents a greater bias on the Tropical Atlantic.

Key words: Wind divergence, wind convergence, scatterometers, ocean surface wind, satellites, MetOp-B, MetOp-C, HY-2B, HY-2C, HY-2D, ASCAT, HSCAT.

Contents

Chapter 1

Introduction

Winds have an undeniable impact in our society, but is also a crucial parameter in the meteorology field and climate system for the understanding physical phenomena and the interactions between the climatic components. They occur because of all the forces acting on air, which are susceptible to moisture, heat fluxes, momentum transfer, Earth's rotation, latitude, orography, friction, etc. The way to understand all these wind dynamics is through observations and models for which satellites have been a game changer during the last years. Throughout this project we will focus on ocean surface wind properties of different scatterometers observation types and numerical weather prediction model fields, which is just a small part of all the wind dynamics.

1.1 Ocean surface wind products and their relevance

Surface winds play a significant role in the understanding of ocean processes and climate research fields, with impacts in energy, momentum and mass fluxes between ocean and atmosphere. These winds influence several mechanisms such as wave generation, sensible heat and CO_2 exchange between air and water. Due to the vast coverage of the ocean over Earth's surface, an extensive comprehension of surface winds is necessary for climate research (Atlas et al. 2011). One of many of these processes affected is water evaporation. Specific heat of the water is considerably higher than the one of land, hence, moisture fluxes associated with oceanic heat loss through evaporation provide an important water source for agriculture and human consumption (Cronin et al. 2019). An accurate quantification of heat and momentum exchange over the ocean surface would make for humans.

Accuracy and resolution are key factors for ocean surface wind products because they directly affect the quality and reliability of weather-forecasting and climate research. Surface winds have a big spatial and time variability, therefore, even with the great availability of observations and models that are present nowadays, it is not an easy task to produce wind products with high accuracy. This sometimes makes Numerical Weather Prediction (NWP) models fail to reproduce the real state of the wind over the surface. To illustrate the impact a reduced model output accuracy can make, we can go back to the events of extreme high tides (Aqua Alta) that occurred in Venice during the days 11-18 of November 2019. During that period, on the 12th of November, the water level reached 1.89m for the first time since 1966. Unfortunately, the official forecast created by the European Centre for Medium-range Weather Forecasts (ECMWF) made an underestimation of almost 40cm for the water level. One of the ways that would help in the prevention of these extreme events in which the surface winds are crucial, would be to have larger quantity and accuracy of wind surface data (von Schuckmann et al. 2021).

1.2 Wind distribution and its interaction with physical phenomena

The global wind patterns are well understood being Earth's rotation, its uneven heating of the surface and the land-water distribution the main drivers of these patterns. All this creates the well-known Hadley, Ferrel and polar cells in both hemispheres which drive the wind patterns in the North-South axis. Moreover, there are also some patterns in the East-West axis influenced by the rotation of the Earth. The rotation makes the Coriolis force which deflects winds to the right in the northern hemisphere and to the left in the southern hemisphere making the trade winds and westerlies to appear. This is just a simplification of the global dynamics so we can understand better the areas of study in this project: the tropical Atlantic and the North Atlantic.

- **Tropical Atlantic**

  At the surface level the tropical Atlantic is driven by the trade winds and the Intertropical Convergence Zone (ITCZ). On the East Tropical Atlantic trade winds blow from the northeast (Northern Hemisphere) and from the Southeast (Southern Hemisphere) converging around the equator where the ITCZ is located. This zone is characterised by a permanent low pressure, high convection, creating cloud coverage and precipitation which affects the energy balance of the Earth (Webster 2020). The incident radiation of the sun is maximum over the equator, but it is blocked by the cloud coverage. The farther we move out of the equator, less incident radiation will reach the top of the atmosphere but, since the cloud coverage is almost non-existent over the tropics, more heat is released from the ocean surface (Waliser & Jiang 2015). See figure 1.1 of a simplified scheme of the Hadley cell.

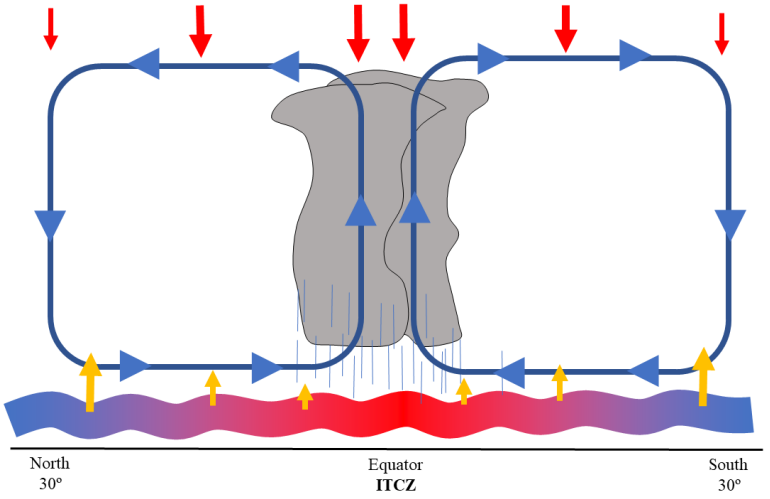

Figure 1.1: Simplification of the Hadley cell with solar incident rays (red arrows), heat transfer from the ocean surface to surface air (yellow arrows), mean wind track (blue circuit) and sea surface temperature (colour gradient of the ocean surface).

- **North Atlantic**
  Regarding the North Atlantic, its surface wind distribution is influenced also by the ITCZ, the Gulf stream and the presence of Tropical and extratropical cyclones among others. As it has been mentioned in the previous paragraph, the Hadley cell has its influence up until 30°N characterising these regions around the latitude 30°N with downward wind and creating wind

divergence over the ocean surface (Webster 2020). Another mechanism with a more localised effect is the sea breeze. This diurnal phenomenon is characterised in this region by a peak of wind divergence over the water surface in the evening around 17:00 – 19:00 Local Sideral Time (LST) (Dai & Deser 1999).

With respect to the ocean, an important phenomenon is the Gulf Stream, located on the western North Atlantic on the coast of the US and Canada. This western boundary current transports heat from the tropics towards the north of the North Atlantic which makes its surface water to be warmer than its surroundings. The higher Sea Surface Temperature (SST) over the Gulf Stream region has multiple impacts on the sea-air interaction. According to Minobe et al. (2008), this current plays a crucial role on the formation of low altitude clouds and cyclogenesis. In addition, the sharp sea surface pressure gradients over the current, lead to surface wind convergence creating lifting of air parcels and eventually rain.

Later, Takatama et al. (2012) showed through modelling that that the primary mechanism for surface convergence over the Gulf Stream is the pressure adjustments mechanism. Regarding the wind divergence, he concluded that the downward momentum mixing is a secondary mechanism. The mechanism of pressure adjustment and downward momentum consist in surface wind convergence (divergence) over the warm (cold) area of an SST front (Gulf Stream in this case).

1.3 Wind divergence and convergence over the surface

This project is focused on the study of wind divergence and convergence of surface wind. The main reason for this choice is that this variable has not been as studied as wind speed and direction although it is still very relevant for many atmospheric processes such as convection, cloud formation or pressure adjustments.

Surface wind convergence refers to the phenomenon where wind from different directions converges or comes together at a specific point or region. It is calculated as the sum of the horizontal spatial derivatives of the wind over the surface (Equation 1.1)

$$\nabla \cdot \vec{V}(x,y) = \frac{\partial u(x,y)}{\partial x} + \frac{\partial v(x,y)}{\partial y} \tag{1.1}$$

The divergence and convergence of surface winds are atmospheric phenomena linked to pressure gradients and temperature. Surface wind convergence occurs when the wind is getting accumulated in a certain region over the surface so the air starts to lift so this lifting air parcels cool down. If the temperature reaches the dew point, condensation will happen and could eventually end up in precipitation.

A known example of wind convergence are the resulting cyclonic winds near the surface in a low pressure system. In this case, the drag force of the surface makes the gradient wind deflect towards where the pressure gradient pushes (Figure 1.2 c)) (Stull 2015). Another important mechanism for this thesis that creates surface wind convergence is convection (Holton 1973).

On the other hand, the surface wind divergence has the opposite mechanism, which is produced when the wind is blowing away from a certain location, usually created by downward wind. It is also related with a high pressure over the surface because of this downward wind (Figure 1.2 d)). However, surface wind divergence can also appear when there is heavy rain because downbursts of wind will descend along with the rain (Holton 1973).

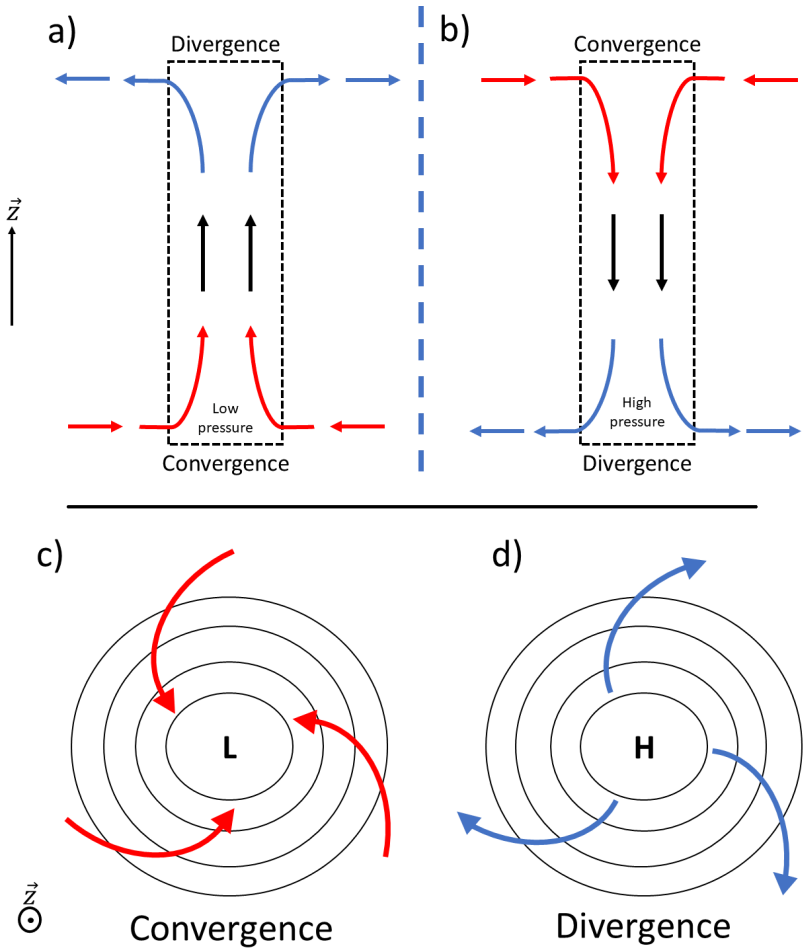

Figure 1.2: Schematic representation of convergence a) and divergence b) seen in the vertical scale and convergence c) and divergence d) over the surface for a low and a high respectively in the northern hemisphere.

1.4 Scatterometers

1.4.1 Evolution of the scatterometers

Scatterometers are crucial to collect information about surface winds over the ocean and without them the understanding of the climate system would have not been as developed as it currently is. It was during World War II when radar backscatter from ships was first used to detect other ships. Later, it was seen that backscatter was more intense for high wind conditions. This eventually led to the use of scatterometers to measure sea surface wind as they do today (Jones 2015). During the late 1960s the National Aeronautics and Space Administration (NASA) started to develop the use of scatterometers from satellites and it was in 1973 when the first satellite carrying a scatterometer was launched. This was the S-193 RADSCAT instrument on the SkyLab satellite. The second scatterometer was put in orbit in 1978 proving scatterometry as a useful technique for research of surface wind with the launch of the SeaSat-A Scatterometer System (SASS) by NASA (Vogelzang & Stoffelen 2012). Its lifetime was just three months but that marked the beginning of the scatterometers as scientific instruments designed to measure ocean surface wind speed. Nevertheless, the boom started in the decade of 1991-2001. This can be seen by the number of observation used by the ERA-40 for that decade where it passed from 0 to 7575 scatterometers observations in use (Uppala et al. 2005) and since then they have been essential for models and

climate research. Table 1.1 offers a review of some of the most important scatterometers missions.

Instrument	**Satellite**	**Mission duration**	**Agency**	Radar Band
SASS	SeaSat	June 1978–Oct1978	NASA	Ku
SCAT	ERS1	July 1991-March 2000	ESA	C
	ERS2	April 1995–September 2011		
NSCAT	ADEOS-1	Aug 1996–June 1997	NASDA	Ku
SeaWinds	QuikSCAT	June 1999–Nov 2009	NASA	Ku
	ADEOS-2	April 2003–Oct 2003	NASDA/NASA/CNES	Ku
ASCAT	MetOp-A	Oct 2006-Nov 2021	EUMETSAT	C
	MetOp-B	Sep 2012 onwards		
	MetOp-C	Nov 2018 onwards		
OSCAT	OceanSat-2	Sept 2009-October 2013	ISRO	Ku
HSCAT	Haiyang 2B	Oct 2018 onwards	CAST	Ku
	Haiyang 2C	Sep 2021 onwards		
	Haiyang 2D	May 2021 onwards		

Table 1.1: Past and present satellites carrying a scatterometer relevant for this project Vogelzang & Stoffelen (2012), European Space Agency (2012), NSOAS (2023).

The information displayed in Table 1.1 will be expanded in Subsection 1.4.3 for the scatterometers used for this project, which are MetOp-B, MetOp-C, Haiyang 2B, Haiyang 2C and Haiyang 2D.

1.4.2 How do scatterometers work

Scatterometers are active radar (microwaves) instruments mounted on satellites that measure the backscatter from the surface of a previously emitted electromagnetic wave. One of the main applications is observation of surface winds over the ocean from satellites. Its mechanism is based on the relationship between the backscatter intensity and the roughness of the sea surface. The more intense sea surface wind is, the more capillary waves driven by this wind will appear intensifying the backscatter (Figure 1.3).

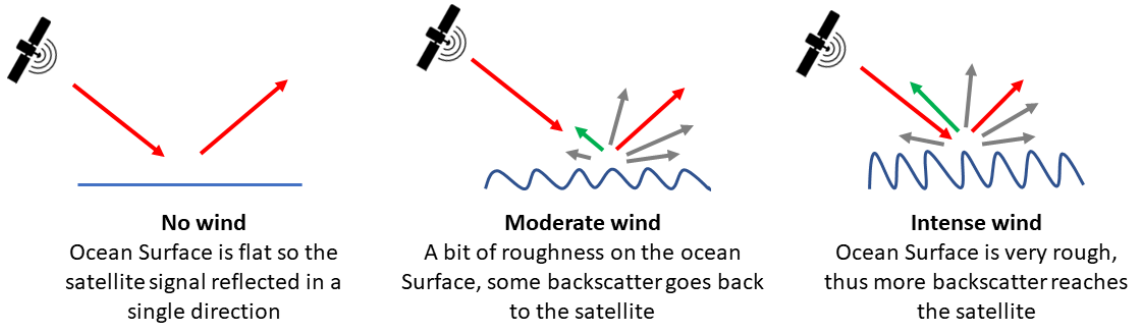

Figure 1.3: Illustration of the backscatter received for no wind, moderate wind and an intense wind configuration.

The physical variable measured by the satellite is the normalised radar cross section of the ocean surface, usually referred to as σ_0 which is dependent on the surface wind and direction. However, other factors affect the σ_0, as the radar frequency and polarisation, incidence and azimuth angle, reflectivity of the surface or presence of land and sea ice. Hence, it is important to know how this influences the measures of the instrument so we can get reliable data (Vogelzang & Stoffelen 2012).

1.4.3 Used satellites and their instruments

This project, which is based on the year 2022, will have acces to two scatterometers instruments, ASCAT, mounted on the MetOp satellites (MetOp-B and MetOp-C) and HSCAT, mounted on the Haiyang satellites (HY-2B, HY-2C and HY-2D). Therefore, there are data available from five different satellites for this thesis. This five satellites will allow to do intercomparison between the same instrument mounted on different satellites and also between satellites with different instruments. As it is seen on the Table 1.1, year 2022 is a crucial year in which a lot of satellites are available at the same time.

There are multiple differences between the satellites, being the main difference the frequency of their scatterometers. ASCAT instruments use the C-band (5.255GHz, $\lambda \approx 5$cm) and HSCAT the K_u band (13.4GHz, $\lambda \approx 2$cm). Nonetheless, there are other differences between the MetOps and the Haiyang satellites as the antenna they use or the swaths of their orbit (see figure 1.4). The differences between the satellites used are described in the table below (see table 1.2)

	Meteorological operational Satellite (MetOp-B, MetOp-C)	Haiyang (HY-2B, HY-2C, HY-2D)
Instrument	ASCAT	HSCAT
Frequency	C-band (5.255GHZ)	K_u-band (13.4 GHz)
Orbit	Sun-synchronus	Sun-synchronous (HY-2B) Non Sun-synchronous (HY-2C and HY-2D)
Antenna	Fixed fan-beam	Rotating pencil-beam
Swath width	2 of 550 km	1800 km
Other	No sensitive to rain	Sensitive to rain Also to higher wind speed

Table 1.2: Comparison between the MetOps and Haiyang satellites used for this project.

As it can be seen in the figure 1.4, the difference between MetOps (ASCAT instrument) and Haiyangs (HSCAT intrument) on the technology used for the antennas is very large. However, in both cases it is needed to measure the backscatter under different incidence and azimuth angles because ultimately the goal is to measure the module and direction of the wind.

The Fixed fan-beam system, which is mounted on MetOp satellites uses two sets of three antennas separated by 45° in each direction except for the direction of the motion (Figure 1.4). They scan the surface of the ocean with two swaths of 550 km width separated by a gap of 670 km. The data have two resolution configuration: high resolution of 12.5 km and low resolution of 25 km. Since the satellite is moving constantly, each point on the surface is going to be scanned three times in a short period of time. Moreover, it only uses beams polarised in the vertical direction (direction of the movement of the satellite) (Nekrasov et al. 2019).

The rotating pencil-beam antenna, used in the Haiyang satellites, is a 1 m parabolic antenna with two offset feeds creating an inner and outer beam by rotating in the plane parallel to the surface. In addition to that movement, the satellite is traveling through space, so the footprint is a wide strip below the trajectory of the satellite and every point is scanned up to 4 times as they can cross twice the outer and inner beams. In contrast to the fixed fan-beam antenna used for ASCAT (MetOp satellites), this one is polarised in the horizontal direction (inner beam) and vertical direction (outer beam) so it is possible to obtain 4 independent measures over the area of the swath (Zhang et al. 2020). The resolution at which the surface is sampled is 25 km so it matches with the "low" resolution of the ASCAT instrument. This type of antenna is often limited to small wavelengths because the benefits of a larger antenna on a rotating system do not match the increase in costs (Vogelzang & Stoffelen 2012).

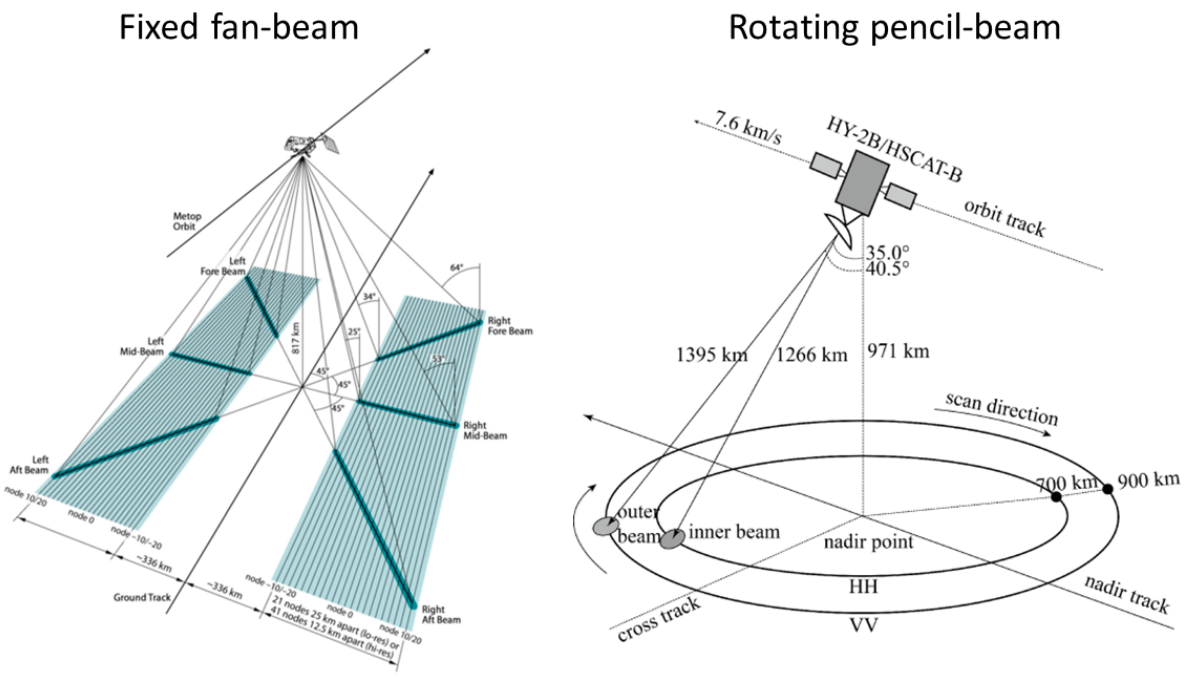

Figure 1.4: Left: Scheme of the fixed fan-beam antenna used on the ASCATs (MetOp satellites) (Nekrasov et al. 2019). Right: Rotating pencil-beam antenna used on the HSCATs (Haiyang satellites) (Zhang et al. 2020)

1.4.4 Processing of the backscatter

As said before, σ_0 is a measure of the cross section and it is defined as the backscattered power divided by the power flux emitted by the instrument, often measured in dB. After taking into account all the geometry of the satellite emission and backscatter, the expression of the Normalised Radar Cross Section σ_0 is:

$$\sigma_0 = \frac{(4\pi)^3 R^4 P_R}{\lambda^2 G^2 P_T} \tag{1.2}$$

With P_T the microwave pulse power, G = 1 for emission in all directions, P_R the backscattered power received by the antenna, F the footprint area covered by the satellite, R the distance between the satellites and the target and λ the wavelength of the emitted beam (Stoffelen 1998).

Once σ_0 is obtained, processing is required in order to obtain the surface wind speed at 10 m over the surface. This processing is possible thanks to the Geophysical Model Function (GMF) which provides the stress equivalent wind speed field at 10 m height (u_{10s}) depending on the incident angle (θ), relative azimuth angle (ϕ), wavelength (λ) and polarisation (ρ) (EUMeTrain 2017)(Stoffelen et al. 2017).

$$\sigma_0 = GMF(u_{10s}, \theta, \phi, \rho, \lambda) \tag{1.3}$$

For practical reasons the wind chosen is at 10 m height because that is the international standard by the World Meteorological Organization. This makes it easier to use them for validation, comparison with other observations and to integrate it with models. Hence, any time throughout this thesis, whenever surface wind is mentioned, it is going to be referred to surface wind processed 10 m over the surface and the same for the wind divergence.

Regarding the variable of the stress equivalent wind obtained after applying the GMF expression, U_{10s}, it is the wind at 10 m over the surface deducted from the backscatter. Surface currents

would influence the creation of capillary waves and hence, the backscatter. Nevertheless, surface currents are not taking into account on wind measurements from scatterometers. That is the reason why the variable used is the stress equivalent wind. It is proportional to the capillary waves created by the wind.

Since the way the backscatter data are obtained depends on a variety of aspects that are different from ASCAT (MetOp satellites) to HSCAT (Haiyang satellites), a separate GMF is required for each of these instruments. In the case of ASCAT the GMF used by the Royal Netherlands Meteorological Institute (KNMI) to process the data is the CMOD7 (Stoffelen et al. 2017) and for HSCAT it is the NSCAT-4DS (Wang et al. 2017) (Wentz & Smith 1999). After the data is processed throughout the GMF function, the variable of wind obtained for the comparison with the ECMWF model output is the equivalent wind stress. Therefore, the neutral wind, which is already an output of the model, is converted to stress equivalent wind (Section 1.5).

1.4.5 Orbits and surface coverage

The orbits define the way a scatterometer covers the surface of the Earth. All the scatterometers used in this project are situated in the Low Earth Orbit, with an altitude close to 900 km-1000 km. The satellites of this project MetOp-B, MetOp-C and HY-2B orbit in a sun-synchronus orbit, while the orbits of HY-2C and HY-2D are not sun-synchronous. Any satellite in a Sun-Synchronous Orbit (SSO) will pass over any point of the Earth at the same local mean solar time (Table 1.3). The ascending node will occur 12 hours later than the descending one. On the contrary, HY-2C and HY-2D have polar inclined orbits which span from 74°N to 74°S. Not having a sun-synchronus orbit means that each day the satellite will change the time at which it passes over a certain region. Observations from this satellites are useful for studying the diurnal cycle (Section 4.10) and for cross validation with other satellites (Eumetsat 2021) (Wang et al. 2021).

	MetOp-B	MetOp-C	HY-2B
Descending node time	9:30	9:30	6:00

Table 1.3: Descending node time for each of the sun-synchronus satellites

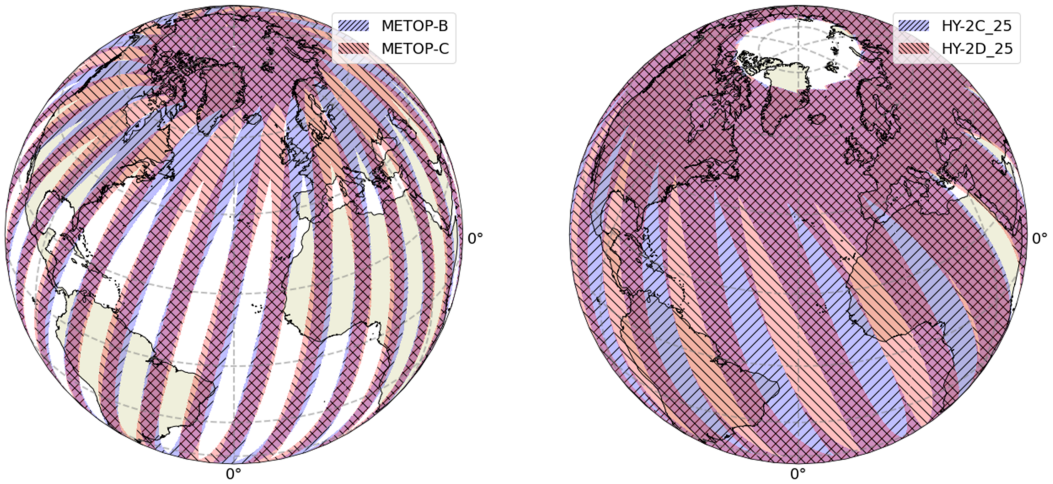

Figure 1.5: Surface coverage in one day of MetOp-B and MetOp-C (left) and HY-2C and HY-2D (right) for the descending node of the orbit

Since these orbits are polar there will be more representation of the Arctic areas than for the

tropics (ESA 2020). Figure 1.5 illustrates that HY-2C and HY-2D coverage spans in a latitude range of 74°N to 74°S with an orbit inclination of 66.0° (Wang et al. 2021). Unlike the other Haiyang satellites, HY-2B describes a polar orbit covering every latitude.

In addition, the satellite instrument setup and configuration, influences the spatial coverage resulting in HSCAT instruments covering a larger fraction of the Earth surface than ASCAT (Figure 1.5). Due to the wider swath of the HSCAT antenna (Section 1.4.3). Furthermore, it is relevant to highlight that MetOp-B and MetOp-C are in phase scanning the same area with a time difference of 50 minutes for the year 2022. These satellites have the same orbit: same descending node (9:30), same inclination, and same period (approximately 101.4 minutes) with the only difference of a phase shift of 50 minutes. This configuration is very useful to study the time scales of phenomena seen by the same instrument (ASCAT) in an interval of 50 minutes (Section 4.8).

1.5 Validation and biases between scatterometers and NWP

A key part of this project is the comparison of scatterometer observations and numerical weather prediction (NWP) fields. NWP fields are generated from weather forecasts made by computers through solving mathematical equations. Since these are complex equations and computers do not have infinity power, it is needed to discretize the model by creating grid cells and finite time steps for solving the equations (Stull 2015). Thus, approximations are taken. The more in the future and the less information of initial conditions, make the forecast to divert from reality.

A direct comparison between surface winds from processed backscatter and models is not possible because the model output does not include the variable stress equivalent wind (U_{10S}). Therefore, U_{10S} is transformed from the neutral wind (U_{10N}) using the ratio of the global averaged air density and the actual air density of each gridpoint (de Kloe et al. 2017) (Eq. 1.4 of the density transformation). A simplified scheme of the data processing for scatterometers and ECMWF model is shown in Figure 1.6.

$$\vec{u}_{10s} = \vec{u}_{10n}\sqrt{\frac{\rho_{air}}{\langle\rho_{air}\rangle}} \tag{1.4}$$

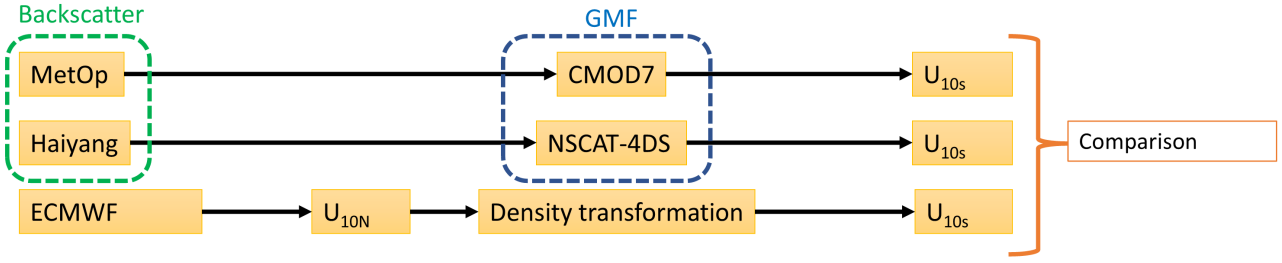

Figure 1.6: Simplified outline of the processing needed to get the stress equivalent wind U_{10S} from the scatterometers and the ECMWF model.

Scatterometers can make a positive impact on NWP model forecasts being used as input or detecting the biases that models have. To achieve that it is very important to understand how the data of the scatterometers is validated and how the model data is collocated so it is possible to compare observations with models. In this thesis the chosen model is the operational model Integrated Forecasting System (IFS) from the ECMWF.

To evaluate the bias of a model with scatterometers, it is needed to have certainty that the data from the scatterometer is accurate. This is the reason why all the datasets of surface wind

from scatterometers pass a extensive quality control and are validated with other observations like buoys as Wang et al. (2020) explains.

1.6 Comparison between NWP and scatterometer observations

Some comparison has already been done between ECMWF and scatterometers winds and between the scatterometers themselves. One of the most complete studies was performed by Wang et al. (2020) getting the following results.

- ASCAT-B and ASCAT-C give almost the same results globally in the validation of wind speed and direction in comparison with buoys.
- Wind speed quality of HSCAT-B is close to the one of ASCAT
- C-Band and Ku-band satellites show different distribution in a probability density plot so a winds speed correction would be needed for the Ku-Band GMF (NSCAT-4)
- ASCAT and HSCAT present similar characteristics of wind speed biases when comparing to ERA5 winds.

Besides this, Belmonte Rivas & Stoffelen (2019) found interesting biases after comparing observations from MetOp satellites to ERA5 and ERA-Interim. This comparison was done in a global scale for the year 2016 and 25km resolution of the satellites.

- ERA zonal winds are excessively westerly in midlatitudes and easterly in the tropics. In addition, they found ERA surface meridional wind to be less intense than the observations in absolute value.
- ERA products are deficient in zonal and meridional surface wind variability mainly over storm tracks.
- In the tropics, ERA products show defective mean convergence over the ITCZ and deficient wind divergence in the subtropical gyres.
- Overall, ERA products show problems with unresolved air flows under conditions of moist convection. This is particularly seen over the ITCZ region and on the warm areas of the Western Boundary Currents (WBC).

Last, King et al. (2022) studied the relationship between extreme convergence and divergence with extremes of rain with 12.5 km ASCAT scatterometer observations. They show how extremes of rain are tied with downbursts of wind and previous convergence for the Tropical Atlantic.

Throughout this project, the bias that is going to be analysed is in the variable of wind divergence and not in wind speed or direction. There is less previous research for the satellites used in this project and the surface wind divergence than for wind speed and direction which makes this variable more interesting due to all the processes that are link to it.

Chapter 2

Project objectives

This project, *Ocean surface wind properties of different scatterometer observation types and numerical weather prediction model fields* is oriented to the analysis of surface wind divergence fields obtained from the satellites MetOp-B MetOp-C, HY-2B, HY-2C and HY-2D. The aims of the project are to improve the understanding of scatterometer wind divergence, to illustrate differences between instruments taking into account physical and technical influences and the identification of ECMWF biases in wind divergence.

The results can be divided in two parts. First, comparison between the satellites and the collocated data from the ECMWF operational model. Having two different families of satellites instruments (ASCAT and HSCAT) will help to determine which are the biases of the model with respect to the observations of the satellites. Second, a comparison between the satellites themselves taking into account the role of the resolution at which they sampled the data, the region that was observed and the timescales of the phenomena observed.

To achieve that, the following specific goals have been established:

- Comparison between satellites and the collocated ECMWF model to identify biases
  - Differences between observations and model.

    How does the distribution of the surface wind divergence differ between scatterometers and the ECMWF model?
  - Correlation between observations and the ECMWF model.

    What is the correlation between the wind divergence obtained by the model and the scatterometers? What is the spatial distribution of these differences? Are the differences significant?
- Surface wind divergence comparison between different scatterometers
  - Distribution of the wind divergence values between different scatterometers and resolution. What are the differences between ASCAT and HSCAT instruments at equal resolution?

    What is the role of the resolution in the observations of wind divergence?
  - Comparison between extremes of wind divergence obtained by MetOp-B and MetOp-C when their swaths overlap.

    Which is the lifetime of the extremes of wind divergence? Do both satellites identify the same event?

All the analyses are going to be done in two different regions: Tropical Atlantic between 25°S and 25°N and North Atlantic between 15°N and 70°N.

The ultimate goal of the project could be presented as the following research questions:

- Which are the main biases of wind divergence of the ECMWF model? Which scatterometer find more biases of the model?
- What are the main differences between the wind divergence values obtained by each of the scatterometers?

Chapter 3

Data and methodology

3.1 Data levels and availability

The entire project is done based on Level 3 data provided by KNMI which has been processed from Level 0. All datasets cover the year 2022 on a global scale with resolutions of 1/8° (12.5 km), 1/4° (25 km) and 1/2° (50 km) depending on the scatterometer (Section 3.1.3) The data processing levels, can be classified from level 0 to level 4 depending on how much the data has been processed (Table 3.1).

Level	Description
0	Raw data at full instrument resolution, reconstructed and unprocessed
1A	Reconstructed, unprocessed instrument data at full resolution, time-referenced, and annotated with ancillary information, including radiometric and geometric calibration coefficients and georeferencing parameters
1B	L1A data that have been processed to sensor units (not all instruments have L1B source data)
1C	L1B data that include new variables to describe the spectra
2	Derived geophysical variables at the same resolution and location as the Level 1 source data
3	Variables mapped on uniform space-time grid scales, usually with some completeness and consistency
4	Model output or results from analyses of lower-level data (e.g., variables derived from multiple measurements), or variables gridded on non-uniform grids, or higher-level data products such as maps and animations

Table 3.1: Brief description of data processing levels for satellite data acquisition (NASA 2021).

3.1.1 Observations wind data processing

Processing from Level 1 to Level 3 has been done by KNMI including already some validation and masking of data that is not reliable. Further information can be found on OSI SAF (2019) Meyer (2016) for the MetOp satellites and OSI SAF Winds (2021) for the Haiyang satellites. After the processing, the data is provided on a regular grid with variety of variables available and collocated ECMWF model variables.

This project focuses on the surface wind divergence which is already provided in the Level 3 data used. Surface wind divergence is calculated as the net sum of the spatial derivatives of the

surface wind (Eq. 1.1).

Therefore, positive values of wind divergence indicate divergence and negative values indicate convergence. Throughout this project, whenever it is said wind divergence, if there is no distinction between convergence and divergence in the same discussion, it will be assumed that wind divergence refers to positive and negative wind divergence, hence divergence and convergence.

Nonetheless, not all the observations have been processed in the same way. At level 1, before the KNMI data processing, 1/8° resolution MetOp observations are applied a top hat filter of 15km on each direction, whereas 1/4° resolution MetOp observations use a Hamming filter that extents 50km to each direction. That is one of the reasons that will explain a different spatial distribution between resolutions of the same scatterometer.

On the contrary, Haiyang satellites use both the same Top Hat filter so no large differences between resolutions of Haiyangs are expected. Top Hat filter consists in a sharp cut filter, on the other hand, a Hamming filter is a gaussian filter, therefore, assuming that all the differences come from the spatial filtering, Haiyang satellites and MetOp 1/8° satellites would present more variability because their filter is narrower and present a sharp cut in comparison with MetOp 1/4°. Some results regarding the spatial differences between MetOps at 1/4° and 1/8° resolution will be presented in section 4.9.

3.1.2 Model data used and collocation process

Comparison between scatterometer observations and model data is one of the main aims of this project. Therefore we require a collocated model in the observation gridpoints and time.

The model used is the Operational Model of the Integrated Forecasting System of ECMWF in its cycle 47r3 for the whole 2022, specifically, the HRES forecasts (High Resolution). More information about this model used can be found on ECMWF (2021).

The collocation of the model data consists in a spatial and time averaging so the output of the model can match the gridpoints and times of the observations. Spatially the resolution of the model used is 9 km. For the collocation, it is averaged using the four nearest neighbours to the gridpoint of collocation. This averaging is weighted as $1/r^2$. This already includes some smoothing of the values, however, taking into account that the resolution of the observations for this project is 12.5 km, 25 km and 50 km, the high resolution provided by the model will not make a significant impact.

With respect to the temporal collocation, the model output is accessed by the collocation process each 3 hours for the MetOp satellites and each 1 hour for the Haiyangs. This difference in the model accessing intervals will impact the results. For that reason, the collocation for HY-2B has also being processed in 3 hour accessing intervals so the influence of the differences between the 1-hourly and 3-hourly model sampling can be studied. In any case, the collocation in time is based on a linear interpolation between the 2 closest available forecasts of the model. As a result of this, some smoothing of the data is included in this processing.

3.1.3 Observations data used

The level 3 data (L3) is provided in NetCDF format. It is available for the year 2022, and for HY-2C and HY-2D just for the first three months (January-March 2022). It is divided in one file per direction of the orbit (ascending or descending) and per day, so it will be easier to analyse both directions separately. That is very important for the sun-synchronous satellites (MetOps and HY-2B) because the direction of the orbit is linked with the local time. Ascending and descending orbits are separated because otherwise there would be overlapping of data observations in each of the files for some areas.

The horizontal resolutions available for the MetOps are 1/8° (12.5 km) and 1/4° (25 km) and for the Haiyangs it is either 1/4° (25 km) or 1/2° (50 km). Datasets of every resolution have to be processed separately. Although the 2022 full year is available for HY-2B at 25 km resolution, for the 50 km resolution only the first three months were processed. Table 3.2.

	0.125° (12.5 km)	0.25° (25 km)	0.5° (50 km)
METOP-B	12 months	12 months	NA
METOP-C	12 months	12 months	NA
HY-2B	NA	12 months*	3 months
HY-2C	NA	3 months	3 months
HY-2D	NA	3 months	3 months

Table 3.2: Available L3 data for this project. All the data is for the year 2022 and the periods of three months correspond to January-March 2022. *For HY-2B the collocated ECMWF model data has been sampled also at 3-hour intervals.

3.2 Methodology

3.2.1 Region selection

Although the availability of the data is global, the areas chosen to analyse in this project are the Tropical Atlantic and the North Atlantic. This will allow us to see the effects of the Gulf Stream, ITCZ and latitude in the biases of the model and in the comparison between observations. The regions are illustrated in Figure 3.1.

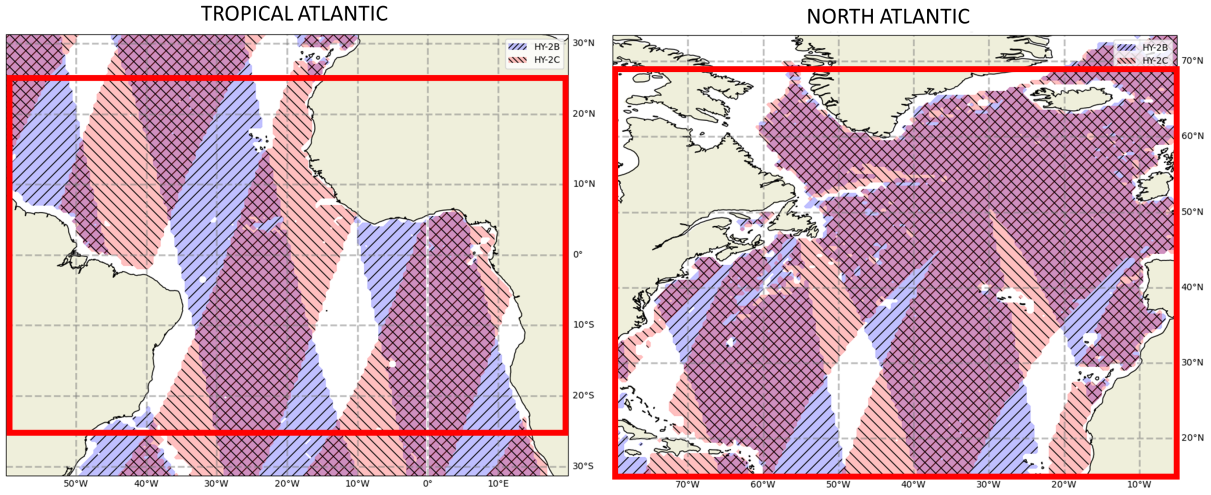

Figure 3.1: Tropical Atlantic (left) and North Atlantic (right) regions illustrated by the availability of HY-2B and HY-2C data of the day 5th of January 2022 as an example. Missing data within the swaths is masked mainly because of interference with rain.

The tropical Atlantic is defined as the region between Africa and the Americas which is in between the latitudes 25°S and 25°N. These Limits are also used in other studies of the tropical Atlantic i.e. King et al. (2022).

For the North Atlantic, the limits are the latitudes 15°N - 70°N and the longitudes 80°W - 0°E. As the non-sun-synchronous satellites HY-2C and HY-2D do not reach higher latitudes than 74°N, 70°N was chosen as the northern boundary. It is also important to remember that any point in

which there is land or ice has been masked so during the winter months there will be some masked data in the northernmost parts of the region.

3.2.2 Statistical Parameters

In order to compare quantitatively the differences between satellites and between them and the collocated model data, some statistics are needed. Mean, standard deviation, skewness and kurtosis will be computed along the project.

- **Mean**
  In this project, the mean is calculated in two different ways. The temporal average wind divergence the mean is calculated as the average values over every gridpoint (x,y) for a predefined period (T), usually one month.

$$\bar{\delta_{T}}_{X,Y} = \frac{1}{T}\sum_{t=1}^{T}\delta_{X,Y,t} \tag{3.1}$$

  With X and Y being longitudes and latitudes respectively.

  The mean is also calculated for the entire dataset, with a the sum over all the dimensions.

$$\bar{\delta} = \frac{1}{T}\frac{1}{X}\frac{1}{Y}\sum_{t=1}^{T}\sum_{x=1}^{X}\sum_{y=1}^{Y}\delta_{x,y,t}\cdot\cos(y) \tag{3.2}$$

  Where δ represents wind divergence and T the total amount of times with data available for each gridpoint. The weight $\cos(y)$ is applied to the mean to avoid the overrepresentation of the gridpoints that are close to the poles because the spatial grid of the data is equispaced in degrees of latitudes and longitudes.

- **Standard deviation**
  Variability of surface wind divergence is a key part of this thesis, it will allow to see how different satellites and the NWP model perceive it. The spatial distribution of the standard deviation is calculated as:

$$\sigma_{x,y} = \sqrt{\frac{1}{T}\sum_{t=1}^{T}(\delta_{x,y,t} - \bar{\delta}_{x,y,T})^2} \tag{3.3}$$

  In parallel to the mean, the standard deviation is calculated by summing also over the desired domain and by applying a latitude dependent weight to balance the overrepresentation of the gridpoints that are closer to the poles.

- **Skewness**
  To measure the asymmetry of the values of each dataset around the mean, we can use the skewness. A negative skewness indicates that the values are skewed to the left and the opposite for a positive skewness. Translating this to wind convergence and divergence would mean that negative skewness is linked to more convergence values and positive skewness with divergence values. Fischer-Pearson skewness coefficient (g_1) is used:

$$g_1 = \frac{m_3}{m_2^{3/2}} \tag{3.4}$$

with

$$m_i = \frac{1}{N} \sum_{t=1}^{T} \sum_{x=1}^{X} \sum_{y=1}^{Y} (\delta_{x,y,t} - \bar{\delta})^i \tag{3.5}$$

- **Kurtosis**
  By using the kurtosis we can describe the "tailedness" of a distribution. Using the Fischer definition of the kurtosis (K), the normal distribution would have a kurtosis of 0. Positive values of kurtosis will mean that the distribution is platykurtic (more tails) than the normal distribution. On the contrary, a negative kurtosis will indicate that the distribution is more leptokurtic (flat tails and high central peak).

$$K = \frac{m_4}{\sigma^4} \tag{3.6}$$

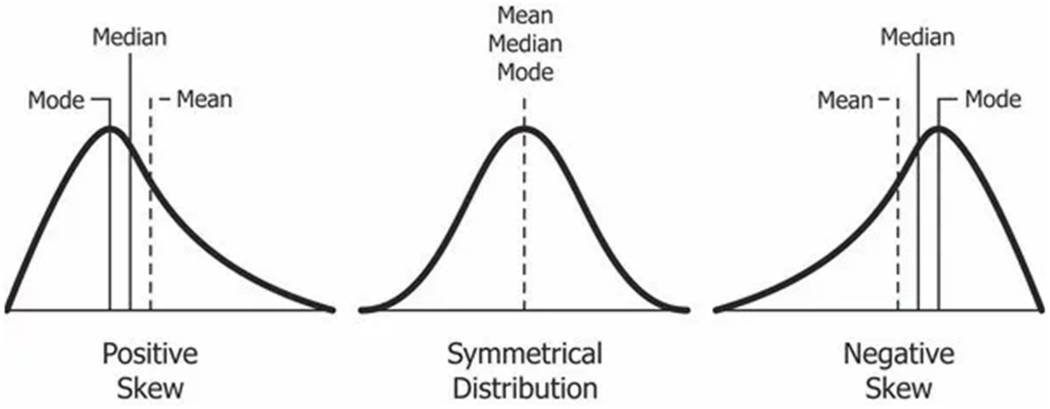

Figure 3.2: Schematic visualization of distributions with different values of skewness (Pipis 2020).

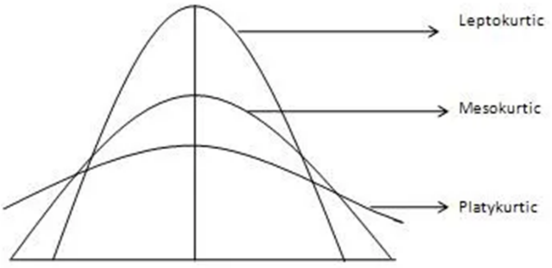

Figure 3.3: Schematic visualization of distributions with different values of kurtosis (Pipis 2020).

Figures 3.2 and 3.3 provide a quantitatively representation of probability density plots for different conditions of skewness and kurtosis respectively.

The calculations of this statistical parameters have been done with the *Python* libraries of *NumPy* (for Mean and Standard deviation) and *SciPY* (for Skewness and kurtosis). With respect to the managing of NaN values, unless the opposite is stated, they have been ignored and all the statistical parameters have been done just with the available real values.

3.2.3 Extremes classification criterion

One of the known biases of the NWP model is that it underrepresents the variability and extremes of the wind divergence (Belmonte Rivas & Stoffelen 2019). For this reason it is important to define what an extreme of wind divergence is.

According to King et al. (2022), any value of wind divergence would be considered as an extreme value if its module is greater than two times the standard deviation of a region. The same criterion is used throughout this project, which will allow us to classify the values in extreme convergence, extreme divergence or neutral conditions. See table 3.3.

Classification	Label	Range
Extreme Convergence	δ_{XC}	$\delta_{XC} < -2\sigma_{region}$
Extreme Divergence	δ_{XD}	$\delta_{XD} > 2\sigma_{region}$
Neutral (background)	δ_{BG}	$\lvert\delta_{BG}\rvert \leq 2\sigma_{region}$

Table 3.3: Followed criteria for the classification of extreme divergence values.

3.2.4 Cumulative Distribution Function

Understanding the distribution of the values for each region and satellite is crucial to start an analysis. In this case, a Cumulative Distribution Function (CDF) is use to visualise the values of every satellite and the collocated NWP. The plots produced showing the CDF contain the variable wind divergence and overlapped we will usually plot the lines that set the boundary between the background values and the extreme values.

This CDF will allow us to see visually how much the wind divergence tails extend and if there is any skewness. If the tails extend farther than a normal distribution the kurtosis is positive. For the skewness, if the values are shifted to the left (convergence) it will be negative. The opposite occurs when they are shifted to the right (divergence). See section 3.2.2 for more information about the statistics. In addition, it is very useful for comparison between satellites between them and with the NWP collocated data.

3.2.5 Satellites - NWP differences

The comparison between the scatterometers and the model is carried in different analyses. Firstly, the statistical parameters and the shape of the CDF for the satellite observations and the collocated NWP values can be compared. However, that would not provide any information about the origin of the biases. Therefore, differences between satellites and models are computed for every gridpoint:

$$\Delta\delta DIF_{x,y,t} = \delta SCAT(x,y,t) - \delta_{NWP}(x,y,t) \tag{3.7}$$

So for every point for which an observation and NWP collocation are available, we can calculate the difference. We then need a way to determine how significant those differences are. For this purpose, correlation and statistical hypothesis testing is introduced.

Alternatively, we can examine the dependency of the scatterometer-model bias on the magnitude of the win divergence. To do so, the available data is divided into intervals (bins) and for each bin the mean difference between the wind divergence value and its collocated NWP model is calculated. We can then compose a plot in which the observation values are on the horizontal axis and the their average difference with the model on the vertical axis. A part of section 4.7 is based on this analysis.

3.2.6 Correlation and Statistical Hypothesis Testing

Correlation is calculated between two datasets with the same amount of values. In most cases it is calculated for comparison between a scatterometer and its collocated NWP value to determine their correlation in a general way. In addition, a spatial correlation map is calculated between a scatterometer and the collocated model value. In this case, we calculate the correlation for each gridpoint with all the values available over the period of interest. Besides that, it is also used in Hovmöller diagrams to examine for which months and latitudes the difference between the model and the scatterometer is significant.

Knowing the correlation already says a lot about the relationship between to group of data, nevertheless, we will perform a statistical hypothesis test to find in which months or gridpoints the model is significantly different from the observations. In all the statistical hypothesis tests done we define a null hypothesis in which the mean value of the data that is being analysed is the same between the scatterometer observations and the model collocations. Besides that, a level of significance (α) is set to 0.01.

$$\begin{cases} H_0 : \mu_{\text{SCAT}} = \mu_{\text{Model}} \\ H_1 : \mu_{\text{SCAT}} \neq \mu_{\text{Model}} \\ \alpha = 0.01 \end{cases} \tag{3.8}$$

As it can be seen from Eq. 3.8, in the previous equation, if the null hypothesis is rejected with a probability lower than 0.01, we can affirm that at a level of significance of $\alpha = 0.01$, the population of the observation and the one from the model are not the same. For some gridpoints the amount of available values is lower than 30, therefore we will use the independence t-student hypothesis test. The software used for this calculation is the function *ttest_ind* from the library *Scipy* in *Python*.

3.2.7 Spatial averaging

In this project the differences between grid resolutions may affect the results. To understand the effect it is useful to reduce the resolution of the datasets with high resolution from 1/8° to 1/4°. The 1/4° gridpoints are exactly in the center of each 4 points of the 1/8° dataset so the averaging will be performed by calculating the mean of the closest 4 points to a 1/4° gridpoint. It is important to take into account that the wind divergence is calculated after the wind speed and direction are computed (Figure 3.4).

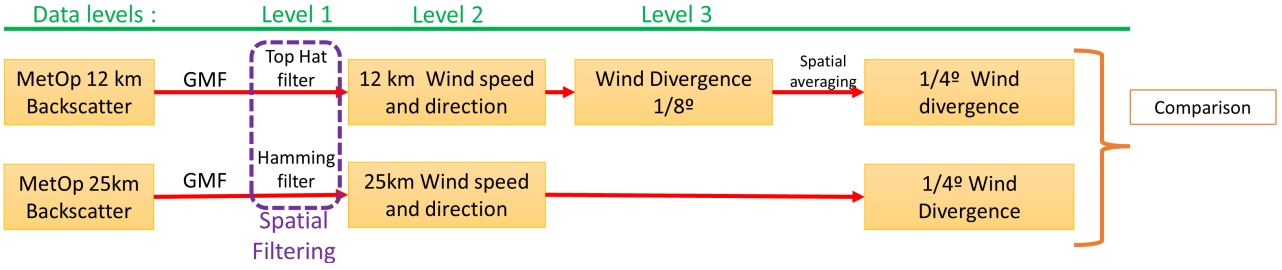

Figure 3.4: Simplification of the processing for wind divergence from 1/8° resolution to 1/4° and its possible comparison with the original 1/4° resolution.

Lowering the 1/8° resolution to match with the 1/4° dataset and its gridpoints, allow us to compare two resolutions from the same satellite and instrument. By doing this, the only effects on the differences will be the resolution and the way the spatial averaging is done.

Note that the MetOps at 12.5 km resolution and at 25 km resolution have been applied a different spatial filtering, therefore, the data is different between resolutions as it was explained in section 3.1.1.

3.2.8 Overlapping areas

Unless the opposite is specified, whenever there is information at different times of the same day for any gridpoint, all the values have been considered. In addition, most of the analyses have been done using the satellites separately and also separating the directions of the orbits (ascending and descending). Allowing for an analysis between directions of every satellite is one of the advantages of the processing from Level1 to Level3 that has been performed at KNMI. On the other hand, when comparing MetOp-B with MetOp-C, the goal is to analyse the areas in which the swaths of the satellites overlap. To achieve this, every gridpoint without information within a time window of around of 50 minutes from both satellites is discarded. This is useful to study of life time of wind convergence and divergence extremes. The constant overlap of the MetOp satellites is not a coincidence, their orbits were planned in a way that one passes after the other within 50 minutes (Figure 3.5).

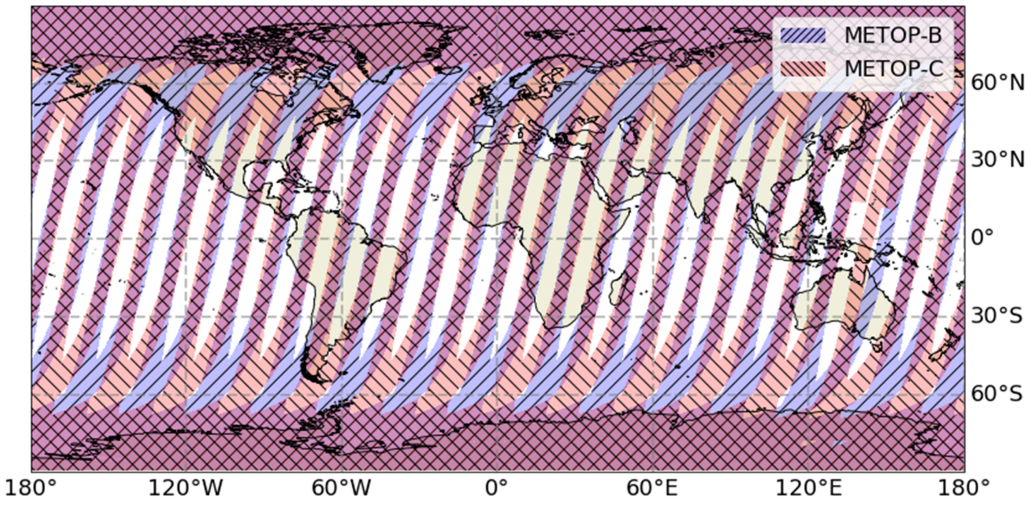

Figure 3.5: MetOp-B and MetOp-C swaths for the 10th of January 2022 in the descending direction of the orbit.

Especially in the tropical areas and the polar regions there is a high proportion of overlap between both MetOp satellites. This does not happen with the Haiyangs but still there are a lot of overlapping areas because their swath is much wider so it covers a larger surface.

Chapter 4

Results

As an introduction to the results on the comparison of wind divergence values with the ECMWF collocated data, Figure 4.1 has been computed. It shows in a global scale observed wind divergence, ECMWF collocated model wind divergence and the difference between them. With respect to the Atlantic, the Tropical Atlantic region shows more differences than the North Atlantic between observations and the collocated model data.

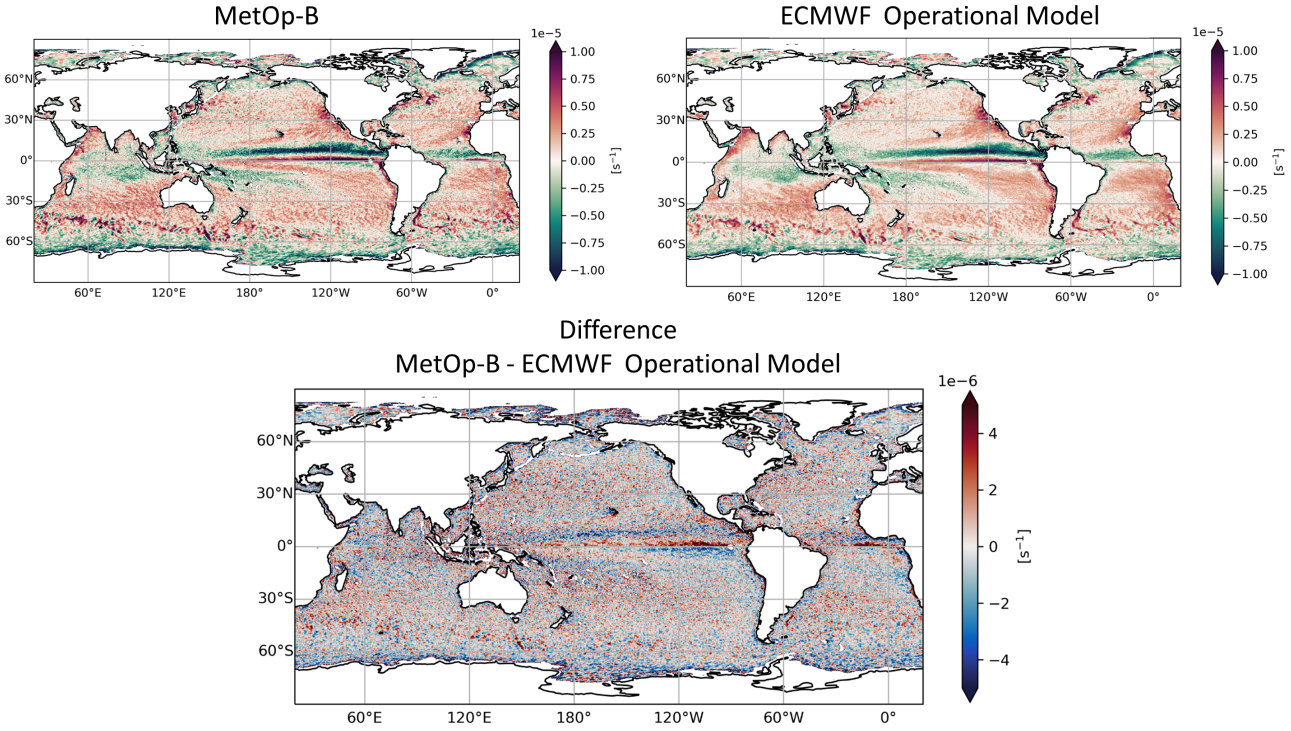

Figure 4.1: Yearly 2022 averaged values of wind divergence from MetOp-B observations, ECMWF collocated model data and the difference between observations and mode.

In this section the results obtained regarding the comparison between the satellites MetOp-B, MetOp-C, HY-2B, HY-2C and HY-2D and its collocated data from the ECMWF model are going to be presented. Secondly, there will also be comparison between satellite observations and their resolution, region and instrument. All the results obtained are regarding the variable wind divergence over the ocean surface.

4.1 ASCAT and HSCAT data distribution

Data collocation and processing is different for the ASCAT and HSCAT instruments (Section 1.4.3). The effect of those differences on the observed wind divergence can be illustrated by creating a CDF plot. There are multiple factors that can influence the data distribution like differences in resolution, instrument, season and region. To support all the CDF plot created for comparison between satellites, standard deviation, skewness and kurtosis has been computed for all the datasets (Table 4.1). CDF plot labels suffix "_25" and "_12" mean $1/4^{o}$ and $1/8^{o}$ resolution respectively (from 25 km and 12.5 km resolution).

Satellites pass at different solar local times, therefore, differences between ascending and descending orbits are influenced by the diurnal cycle (section 4.10). In any case, there are some patterns between satellites worth to analyse regardless the direction. To make the presentation more clear we will only show results for the descending orbit. Even so, for every plot displayed, both directions have been checked and their statistical parameters are included in tables.

- **All satellites at 1/4° resolution**
  Wind divergence from ASCAT and HSCAT observations is compared at 1/4° because this resolution is available for all five satellites. the study period is restricted to January-March 2022 because data for HY-2C and HY-2D is only available for these three months (Table 3.2).

  The CDF plots for all satellites and both North Atlantic and Tropical Atlantic regions (Figure 4.2) shows in both regions a clear asymmetry between extreme convergence (left tails) and divergence (right tails). In both regions, the data distribution is grouped into two different groups which correspond to the ASCAT instrument (MetOp satellites) and HSCAT instruments (Haiyang satellites). The observations from MetOp satellites tend to be more scattered and have more prevalence of extremes, this is also noticeable from the greater 2σ extension for the MetOps. This difference between the instruments is most clearly visible for the convergence (negative tail) in both regions. The extreme values of divergence for the Tropical Atlantic region are closer between MetOps and Haiyangs. To summarise, there is a high proportion of extremes value for both instruments and regions and MetOps present slightly more extreme values than Haiyangs in both regions and for convergence and divergence. This is consistent with what it is seen on the positive kurtosis of table 4.1. There is no noticeable difference between satellites with the same instruments.

- **ASCAT Satellites 1/8° and 1/4° resolution**

  ASCAT satellites (MetOp-B and MetOp-C) processing provides data at two different resolutions (Section 1.4.3), therefore it is possible to compare the result between satellites with the same instrument on board (ASCAT) to visualise what the role of the resolution is. See the CDF plots in Figure 4.3 for the same period as before (January-March 2022) and in the same regions: North Atlantic and Tropical Atlantic.

  The four plots represented in Figure 4.3 reveal the influence of the resolution in the data distribution. In addition, there is almost no difference between the satellite MetOp-B and MetOp-C. For the high resolution observations (1/8°) there is more representation of extreme values of convergence (negative tails) and divergence (positive tails) than for the observations at 1/4° resolution.

  Since the resolution plays such a big role, it is not possible to see any other effect, therefore a normalisation has been done to minimize the effect of resolution difference. After dividing every dataset by its value of standard deviation σ, the difference between the two resolutions almost vanishes (see normalised subplots in figure 4.3). The red vertical lines that are present

North Atlantic	Resolution	Direction	MetOp-B	MetOp-C	HY-2B	HY-2C	HY-2D
Standard Deviation (s^{-1})	1/8°	ASC	5.42E-05	5.38E-05	NA	NA	NA
		DES	5.61E-05	5.56E-05			
	1/4°	ASC	3.02E-05	2.99E-05	2.71E-05	2.74E-05	2.73E-05
		DES	3.16E-05	3.10E-05	2.70E-05	2.70E-05	2.70E-05
	1/2°	ASC	NA	NA	1.97E-05	2.00E-05	1.99E-05
		DES			1.98E-05	1.95E-05	1.96E-05
Skewness	1/8°	ASC	-1.35	-1.42	NA	NA	NA
		DES	-1.29	-1.10			
	1/4°	ASC	-2.21	-2.30	-1.51	-1.58	-1.54
		DES	-2.48	-2.14	-1.55	-1.51	-1.67
	1/2°	ASC	NA	NA	-1.92	-2.22	-2.06
		DES			-2.05	-2.04	-2.32
Kurtosis	1/8°	ASC	19.64	21.42	NA	NA	NA
		DES	19.67	16.48			
	1/4°	ASC	30.28	30.25	14.94	15.89	15.55
		DES	31.95	28.16	15.88	15.28	17.43
	1/2°	ASC	NA	NA	16.03	20.82	17.22
		DES			17.20	17.62	22.27

Tropical Atlantic	Resolution	Direction	MetOp-B	MetOp-C	HY-2B	HY-2C	HY-2D
Standard Deviation (s^{-1})	1/8°	ASC	4.18E-05	4.14E-05	NA	NA	NA
		DES	4.71E-05	4.72E-05			
	1/4°	ASC	2.08E-05	2.06E-05	2.02E-05	2.03E-05	2.07E-05
		DES	2.27E-05	2.28E-05	2.10E-05	1.99E-05	2.00E-05
	1/2°	ASC	NA	NA	1.27E-05	1.28E-05	1.30E-05
		DES			1.32E-05	1.26E-05	1.26E-05
Skewness	1/8°	ASC	-0.47	-0.58	NA	NA	NA
		DES	-0.27	-0.30			
	1/4°	ASC	-0.73	-0.91	-0.32	-0.45	-0.43
		DES	-0.76	-0.71	-0.38	-0.32	-0.40
	1/2°	ASC	NA	NA	-0.53	-0.75	-0.60
		DES			-0.64	-0.54	-0.54
Kurtosis	1/8°	ASC	19.86	22.51	NA	NA	NA
		DES	16.67	15.34			
	1/4°	ASC	23.02	23.43	11.32	8.71	8.66
		DES	14.98	14.64	8.23	8.53	9.38
	1/2°	ASC	NA	NA	11.26	7.18	8.39
		DES			7.61	8.74	8.13

Table 4.1: Statistical parameters for all the datasets available computed for North Atlantic and Tropical Atlantic regions for the time period January - March 2022. Colour scale goes from minimum (blue) to maximum (red) and it is re-scaled with the maximum and minimum value for each statistical parameter.

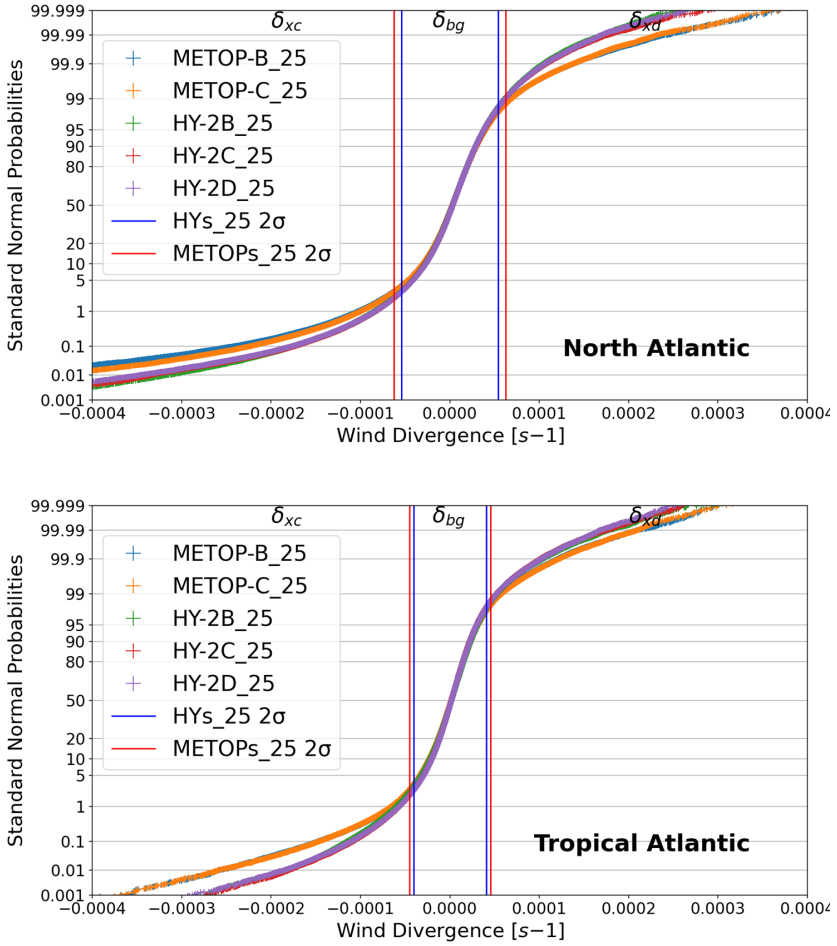

Figure 4.2: CDF plot of surface wind divergence values computed for the months Januray - March 2022 for the North Atlantic (up) and Tropical Atlantic (down). 2σ threshold as an average of the MetOps (red line) and Haiyangs (blue line).

in the normalised subplots just represent the values "2" because after dividing the datasets by their own standard deviation, we can use 2 as the threshold for extreme values.

Regarding the data distribution of the MetOp satellites, the normalised plots show that the extreme convergence values are more "extreme" than the divergence ones. In other words, there are more and higher absolute values on the left tail of the CDF than on the right which Illustrates that the negative skewness of the observations (Table 4.1). Furthermore, there are more extreme values of convergence for both satellites and resolutions in the North Atlantic region than in the Tropical Atlantic region. This is also seen in the more negative skewness for the North Atlantic region (Table 4.1).

- **HSCAT Satellites $1/4^{o}$ and $1/2^{o}$ resolution**

  HSCAT satellites observations (HY-2B, HY-2C and HY-2D) in are available in two different resolutions, 1/4° and 1/2 (1/4° and 1/2° respectively) for the same period of January-March 2022. Figure 4.4 provides a comparison in CDF plots of the satellites HY-2B, HY-2C and HY-2D.

  Although there are some subtle differences between satellites at the same resolution (Figure 4.4 and Table 4.1), data froom all the three satellites have almost the same distribution.

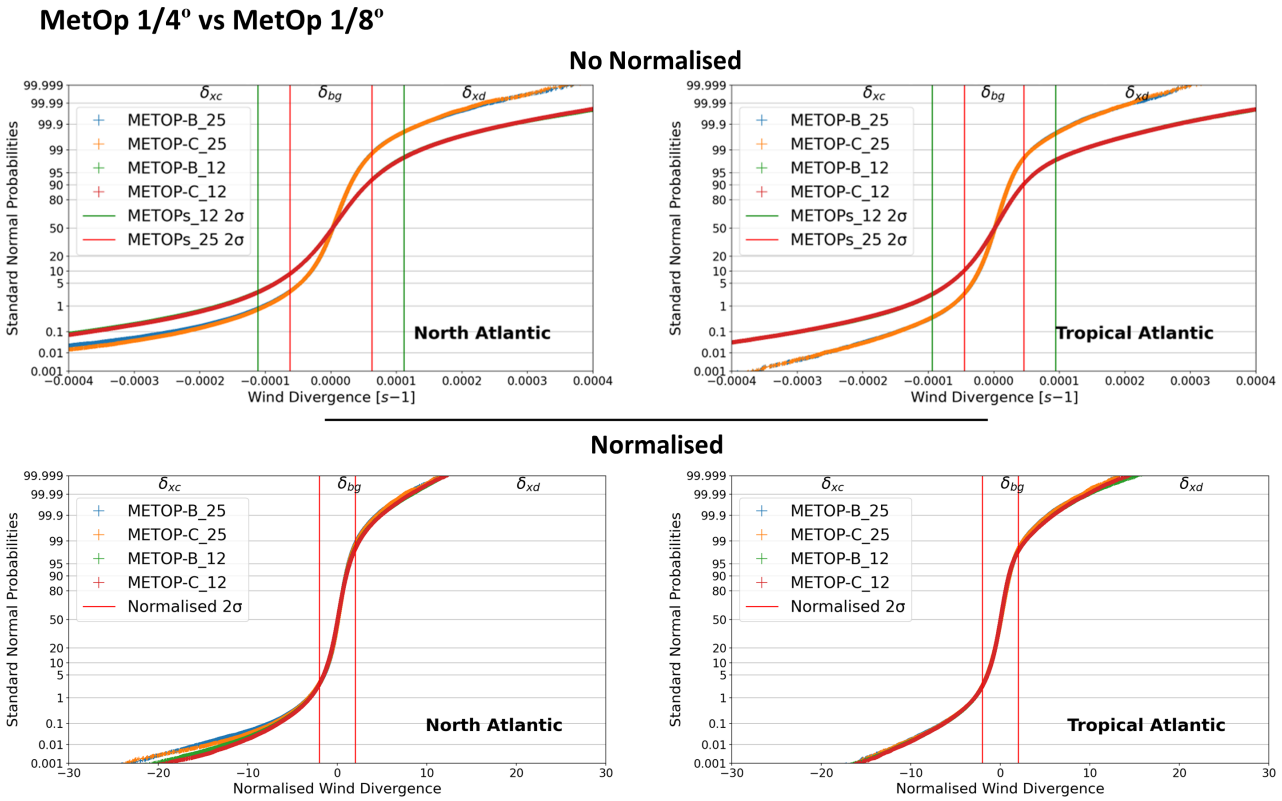

Figure 4.3: CDF plot of surface wind divergence values from ASCAT instruments computed for the months January - March 2022 for the North Atlantic (left) and Tropical Atlantic (right) without normalisation by σ data (up) and with normalisation (down). 2σ thresholds are indicated with solid lines. The suffixes "_25" and "_12" indicate the resolution of the dataset (25 km and 12.5 km respectively)

Again, more differences between resolutions are found on the tropical Atlantic than in the North Atlantic and for the North Atlantic there are more values of extreme convergence than for the Atlantic which denotes a more negative skewness for the North Atlantic region.

The comparison between ASCAT and HSCAT instruments and the resolutions available for the period January-March 2022, has revealed a number of consistent patterns consistent patterns have been observed. These patterns can be summarized in the following list:

- High resolution observations contain a higher proportion of extreme values compared to lower resolution datasets.
- Differences between satellites with the same instrument are not visible for MetOp satellites and almost non-existent for Haiyang satellites.
- ASCAT observations present more extreme values than HSCAT ones.
- For every satellite, there are more extreme values in the North Atlantic region, especially in convergence (negative values).
- For every resolution, region and instrument, there is negative skewness and positive kurtosis (More convergence than divergence and high presence of extremes) (Table 4.1).

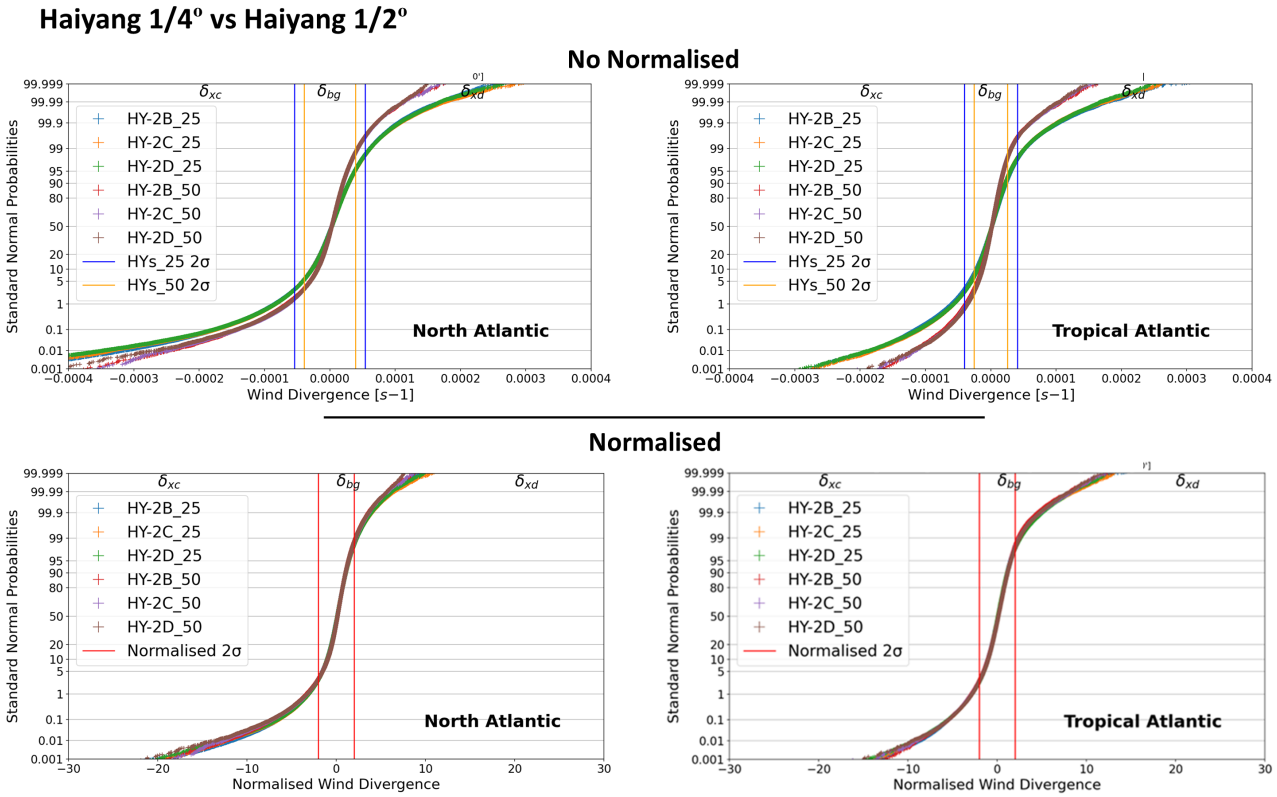

Figure 4.4: CDF plot from HSCAT instruments of surface wind divergence values computed for the months January - March 2022 for the North Atlantic (left) and Tropical Atlantic (right) with normalised data. 2σ thresholds are indicated with solid lines.

4.2 Scatterometer observations and collocated NWP data distribution

All the datasets are provided with the corresponded collocated data in the same gridpoints and time as the observations. That makes it possible to compare the data distribution of the observations with the NWP coming from the ECMWF model. For the following comparison the time interval is fixed again at January-March 2022 because it is the longest period of available data for which we have information from all the satellites.

- **MetOp satellites - NWP**

  Since the differences between MetOp satellites are very small (Section 4.1), we will only show MetOp-B of the ASCAT instrument satellites. We will compare the high resolution ($1/8^{o}$) MetOp-B to MetOp-B of $1/4^{o}$ resolution. Doing that will allow us to compare the collocated data at different resolutions and also to compare it with the MetOp-B observations.

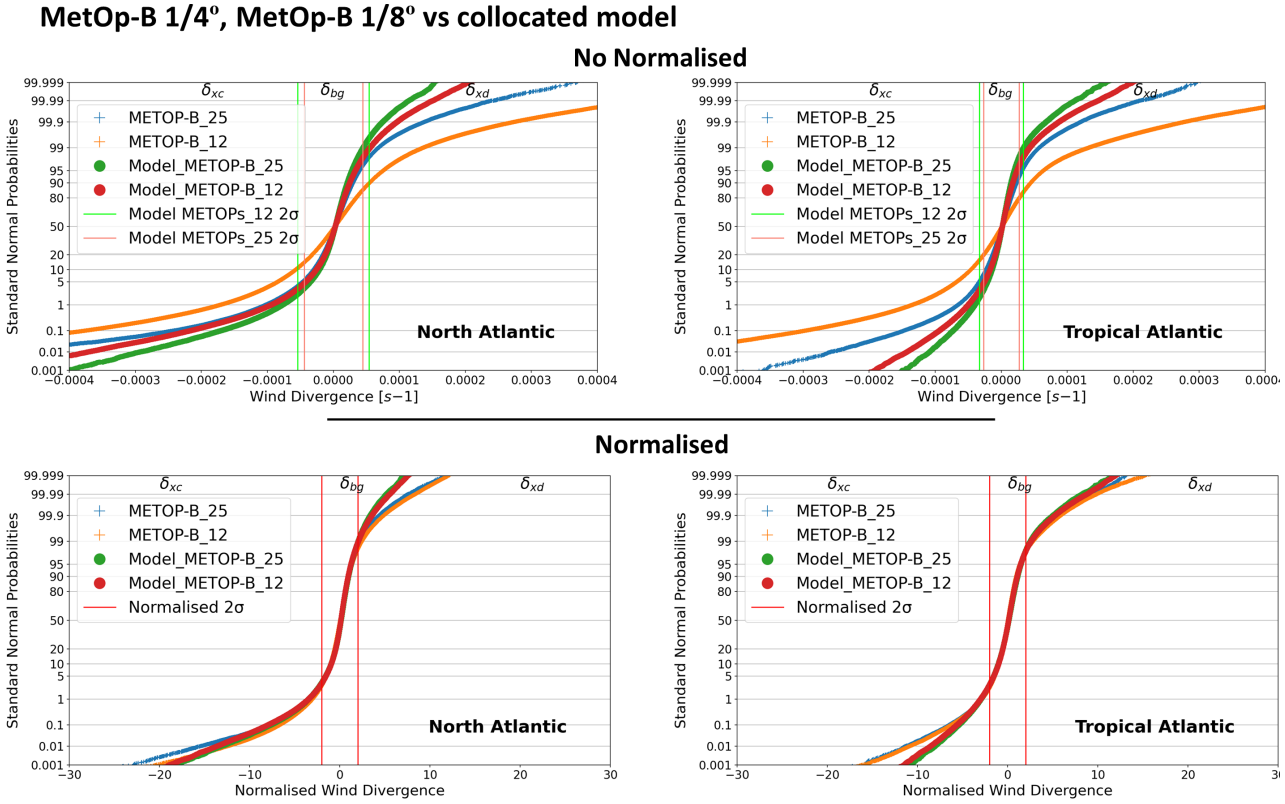

Figure 4.5: CDF plot of MetOp-B at $1/4^{o}$ and $1/8^{o}$ resolution and their collocated data of surface wind divergence values computed for the months January - March 2022 for the North Atlantic (left) and Tropical Atlantic (right) with no normalised by σ data (up) and normalised (down). 2σ thresholds are indicated with solid lines.

In the figure 4.5 the surface wind divergence observations of MetOp-B are represented at 12.5 km and 25 km resolution with its collocated data. The results for the observations are exactly the same as we saw in the previous section but now we can use them as a reference to compare with the collocated data.

The first noticeable thing in the no normalised CDF plots (Figure 4.5) is that the collocated data of different resolutions do not overlap. The higher the resolution is in the collocated

model, the more extremes we find, so the model seems to be reproducing more small scale phenomena which makes the tails to be longer for the high resolution collocation. The difference between the distribution of collocated data that comes from the same model can just be explained by the role of the resolution of the gridpoints to which the data was collocated. Therefore, a normalisation of all the data is required to remove the effect of the resolution.

Looking at the two normalised CDF plots (figure 4.5) we see the effect of the difference in resolution removed because the collocated data with a resolution of $1/8^{o}$ matches with the one of $1/4^{o}$ resolution. In addition, the difference between observations at different resolutions is also very small, the normalised plots for both regions show how observations almost overlap. Nevertheless, in the normalised plots, there is a big difference between the observations and the collocated model. Consistently the data distribution of the model is showing less variability (driven by the standard deviation) than the observations. Besides that, especially for the wind divergence, the collocated values present less extreme values than the observations.

With regard to the region, the biggest difference between model and observations is seen in the North Atlantic for the wind divergence. On the contrary, the difference in convergence between observations and model in the North Atlantic is very small. It is in the Tropical Atlantic where we find a large difference in the wind convergence with the model, again with the model showing less variability in comparison with the observations.

- **Haiyang satellites - NWP**

  Similar analysis is carried out for the Haiyang satellites to compare the data distribution to the collocated ECMWF model. As seen in the previous section, data distribution between different HSCAT satellites was almost the same (Figure 4.4), therefore, for simplicity, in this analysis, the plots will only contain observations from HY-2B in $1/4^{o}$ and $1/2^{o}$ resolution (Figure 4.6). The analysis has been performed for HY-2C and HY-2D with comparable results, also for their collocated model.

  The data distribution in the figure 4.6 shows us a similar result as the comparison between Metop-B and its collocated model. HY-2B collocated data is also influenced by the resolution, the higher the resolution, the more variability the data. Regarding the difference between regions it has the same pattern as seen in the other comparisons, more variability in the North Atlantic, especially for convergence and negative skewness.

  Regarding the normalised data, the difference between the collocated data is non existent but between the observations and the collocated data a small difference can be noticed. Even in the normalised data distribution, the collocated data has a bit less of extreme values than the observations. In any case, HSCAT observations are closer to collocated data than ASCAT.

Table 4.2 presents quantitatively the statistical parameters that support the ideas discussed of the CDF plots regarding the distribution of the observations of MetOp-B and HY-2B and their collocated model data. It important to remark that the differences between the collocated model data between ASCAT and HSCAT is that ASCAT has been collocated with a 3-hour accessing intervals and HSCAT with 1-hour. Therefore, ASCAT collocated data is more averaged in time (Section 3.1.2)

The comparison regarding the data distribution of the observations with the NWP collocated data provides some interesting results:

- The resolution of the observations also influences the NWP collocated data distribution, this effect is mostly removed after normalising the data.

North Atlantic	Resolution	MetOp-B	**MetOp-B Model**	HY-2B	**HY-2B Model**
Standard deviation (s^{-1})	$1/8^{o}$	5.61E-05	**2.71E-05**	NA	NA
	$1/4^{o}$	3.16E-05	**2.21E-05**	2.70E-05	**2.26E-05**
	$1/2^{o}$	NA	NA	1.98E-05	**1.72E-05**
Skewness	$1/8^{o}$	-1.29	**-2.65**	NA	NA
	$1/4^{o}$	-2.48	**-2.53**	-1.55	**-1.62**
	$1/2^{o}$	NA	NA	-2.05	**-1.95**
Kurtosis	$1/8^{o}$	19.67	**23.16**	NA	NA
	$1/4^{o}$	31.95	**20.98**	15.88	**14.42**
	$1/2^{o}$	NA	NA	17.20	**15.73**

Tropical Atlantic	Resolution	MetOp-B	**MetOp-B Model**	HY-2B	**HY-2B Model**
Standard deviation (s^{-1})	$1/8^{o}$	4.71E-05	**1.66E-05**	NA	NA
	$1/4^{o}$	2.27E-05	**1.35E-05**	2.10E-05	**1.74E-05**
	$1/2^{o}$	NA	NA	1.32E-05	**1.18E-05**
Skewness	$1/8^{o}$	-0.27	**-0.44**	NA	NA
	$1/4^{o}$	-0.76	**-0.48**	-0.38	**-0.41**
	$1/2^{o}$	NA	NA	-0.64	**-0.58**
Kurtosis	$1/8^{o}$	16.67	**8.31**	NA	NA
	$1/4^{o}$	14.98	**6.89**	8.23	**7.36**
	$1/2^{o}$	NA	NA	7.61	**5.39**

Table 4.2: Collocated data statistical parameters for MetOp-B and HY-2B. Observations are also include for comparison. they are the same as in Table 4.1. Descending orbits January-March 2022. Colour scale goes from minimum (blue) to maximum (red) and it is re-scaled with the maximum and minimum value for each statistical parameter.

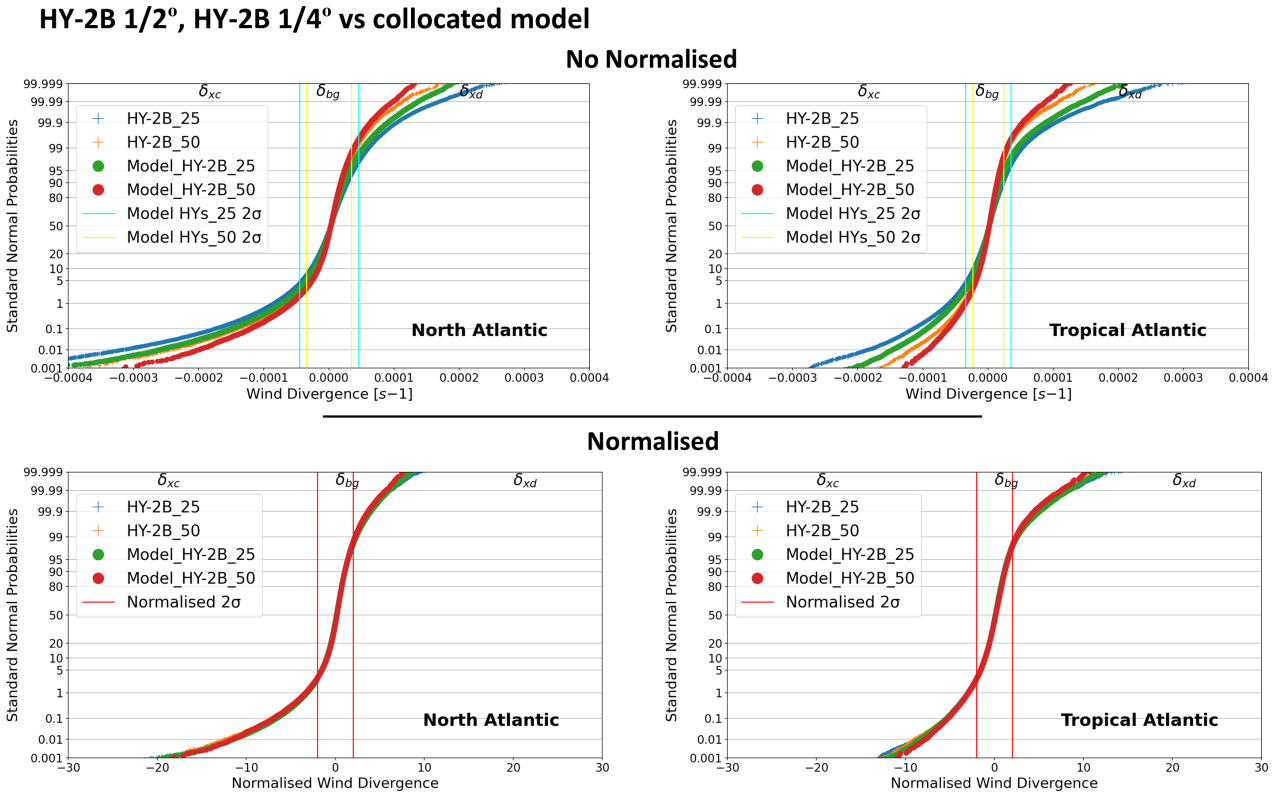

Figure 4.6: CDF plot of HY-2B at 1/4º and 1/2º resolution and their collocated data of surface wind divergence values computed for the months January - March 2022 for the North Atlantic (left) and Tropical Atlantic (right) with no normalised by σ data (up) and normalised (down). 2σ thresholds are indicated with solid lines.

– For the extreme values there are significant differences between MetOp observations and their NWP collocated data, even after normalising the data. Some differences are found also between Haiyang satellites and its collocated data but to a smaller extent than for the MetOps. Table 4.2 reflects the differences of normalised data on skewness and kurtosis.

4.3 Evolution of statistical parameters in the year 2022

The majority of the results from the previous two sections can be quantified using standard deviation to assess the data's variability, skewness to determine the distribution's asymmetry, and kurtosis to examine the shape of the distribution (Table 4.1). A negative skewness indicates more wind convergence (negative wind divergence) and a positive kurtosis suggests more extremes values in the distribution.

In this section we analyse these statistical parameters for every month of the year 2022 for the satellites MetOp-B and HY-2B with their collocated data. The resolutions chosen for this are 1/8º and 1/4º (1/8º resolution is only available for the MetOp satellites). The resolution of 1/2º from the Haiyang satellites has been discarded because the data is not available for the whole year (Table 3.2). All the results of the evolution of statistical parameters have been computed for all the satellites available, the only reason to just use MetOp-B and HY-2B are shown because the differences between satellites of the same family were minimal. In addition, it is important to remember that for this graph we use the collocated data sampled 3-hourly for all the collocated

datasets (MetOp-B and HY-2B) so there is no difference in the accessing interval to the model output and the smoothing that the interpolation between model output can create.

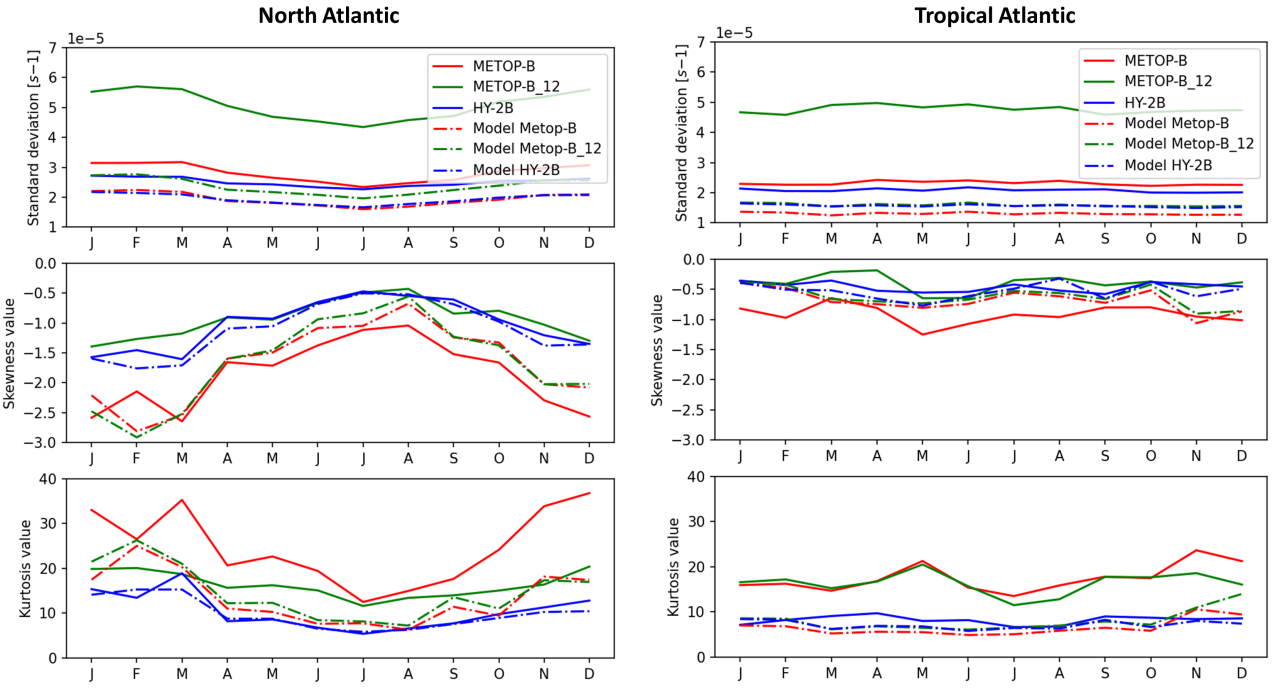

Figure 4.7: Evolution of the statistical parameters standard deviation (up), Skewness (middle) and kurtosis (down) for the wind divergence in the regions North Atlantic (left) and Tropical Atlantic (right) for the year 2022. Data from orbits in the descending direction.

Figure 4.7 presents the evolution throughout the year 2022 of the standard deviation, skewness and kurtosis. In line with the results (Section 4.2), collocated model data has a smaller standard deviation which means that the values display less variability.

Comparing the two regions we find a pronounced seasonal cycle for the North Atlantic whereas in the Tropical Atlantic there is no clear seasonal influence. With just one year of data it is not possible to draw conclusions in a climaologically sense but we could attempt to explain the differences between the North Atlantic and the Tropical Atlantic.

During the winter there are more phenomena that affect the variability (standard deviation) in the North Atlantic such as the occurrence of winter storms. On the other hand, there is no visible seasonal variability in the parameters describing the Tropical Atlantic. That does not mean that there is no seasonal cycle, because it is well-known how the ITCZ shifts during the year. The reason that this seasonal cycle is not seen is that the data is collected in the region between 25°N and 25°S and the ITCZ shifts within this latitudes interval.

Regarding the skewness and kurtosis, they indicate that for the summer months there is less prevalence of convergence (negative skewness) in comparison with winter months. In other words, less surface wind convergence is found in the summer for the North Atlantic. That could be explained due to the amount and strength of convergent systems, such as low pressure systems, which are more common during winter than during the summer. The same happens with the proportion of extreme values (kurtosis). A higher kurtosis is found in during the winter than during the summer, which indicates that extreme values occur more often in the winter months.

Another interesting result from Figure 4.7 are the differences between observations. As analysed in Section 4.1, the higher the resolution is, the greater the variability (standard deviation) is found.

This can be perfectly seen in the differences between the observations of the MetOp-B at $1/4^{o}$ resolution and the MetOp-B at $1/8^{o}$ resolution. In the case of the HY-2B, it presents less variability than the MetOp at the same resolution ($1/4^{o}$) as it was also seen in the Figure 4.2.

Regarding skewness and kurtosis, the results are consistent with what it was described in Section 4.1. HSCAT wind divergence has less skewness and less kurotsis, therefore, they present a data distribution closer to a normal distribution than ASCAT. There is also a big difference between the two resolutions of MetOp satellites. High resolution MetOp-B ($1/8^{o}$) has less skewness and kurtosis than $1/4^{o}$ resolution MetOp-B for every month which could be explained by the different spatial processing (Section 3.1.1). Further analysis in this differences will be done in the section 4.9.

With respect to the differences between the observations and the collocated data from the model, it is found that the high resolution ($1/8^{o}$) MetOp-B observations show the lowest correspondance with the collocated model data. On the contrary, HY-2B observations usually have a comparable values of the three statistical parameters reviewed regardless the region or the season. As a general result, the collocated data (in dashed lines) is closer to the normal distribution parameters. In other words, the standard deviation is closer to 1 than the observations, and for the skewness and kurtosis is closer to 0 if we compare it with the data from the satellites.

4.4 Correlation between observations and their NWP collocated data

Distribution plots allow for a comparison of the data distribution in datasets which may cover different regions, different times of the day or have different resolution. However, similar distribution may do not imply that the events shaping these distributions occurred in the same place and the same time. On the other hand, correlation provides a way to measure if the modeled wind divergence is showing a linear relationship with the observed wind divergence. For all the 5 satellites (MetOp-B, MetOp-C, HY-2B, HY-2C and HY-2D) we calculated the correlation with their collocated NWP data (Table 4.3). All available resolutions have been used for the time interval January to March 2022 because that is the only time interval in which all the satellites have available data.

Region	Resolution	Direction	MetOp-B	MetOp-C	HY-2B	HY-2C	HY-2D
North Atlantic	$1/8^{o}$	ASC	**0.06**	**0.06**	NA	NA	NA
		DES	**0.07**	**0.06**			
	$1/4^{o}$	ASC	**0.18**	**0.15**	**0.51**	**0.46**	**0.48**
		DES	**0.16**	**0.17**	**0.46**	**0.43**	**0.43**
	$1/2^{o}$	ASC	NA	NA	**0.68**	**0.63**	**0.64**
		DES			**0.69**	**0.64**	**0.69**
Tropical Atlantic	$1/8^{o}$	ASC	**0.01**	**0.01**	NA	NA	NA
		DES	**0.01**	**0.01**			
	$1/4^{o}$	ASC	**0.04**	**0.04**	**0.30**	**0.29**	**0.29**
		DES	**0.03**	**0.03**	**0.29**	**0.28**	**0.25**
	$1/2^{o}$	ASC	NA	NA	**0.42**	**0.41**	**0.41**
		DES			**0.42**	**0.40**	**0.37**

Table 4.3: Correlation between observations and their collocated NWP data. Data from January-March 2022. Colour gradient goes from the minimum values (red) to the maximum values (green). "ASC" and "DES" indicate Ascending and Descending orbit direction.

Table 4.3 shows that there is no significant difference between orbit directions, neither between

instruments with the same technology and data processing. All the results for the MetOp satellites (ASCAT) are similar between them and the same occurs with the Haiyangs (HSCAT). However, there are significant differences between regions, resolutions and scatterometer instruments (ASCAT vs HSCAT).

Differences between regions

North Atlantic observations present higher correlation with the collocated data than those for the Tropical Atlantic region. This could indicate that the model performs better in the North Atlantic than in the Tropical Atlantic. Previous literature analysing the biases of the model point out that the model ECMWF has larger wind divergence biases over the tropical areas than over the midlatitudes (Belmonte Rivas & Stoffelen 2019).

Differences between resolutions

The previous sections have shown that the higher the resolution is, the more variability and extreme values are found. As it was seen in Section 4.2, the data distributions closest to to model were the ones with low resolution. The model does not resolve as well the small scale phenomena as Belmonte Rivas & Stoffelen (2019) discovered and those small scale phenomena are more present in the high resolution observations.

Differences between scatterometer instruments

There is clearly a higher correlation between Haiyang (HSCAT) satellites and their collocations than between the MetOp satellites (ASCAT) and their collocated NWP. However, there is a difference between the collocated data from the Haiyangs and the MetOps that could influence the correlation. Haiyang satellites have collocated model data interpolated from a 1-hourly output of the ECMWF model whereas MetOp satellites get the collocated model data interpolated from a 3-hourly output of the ECMWF model which will influence the correlation between observations and the collocated model. On the other hand, it has been shown in the previous sections that the HSCAT instruments do not show as much extreme values as the MetOps. This could make them agree more with the model because the model does not correctly represent extreme values (Belmonte Rivas & Stoffelen 2019).

Furthermore, although Table 4.1 showed some subtle differences between ascending and descending direction, in the correlation the differences are non-existent. Differences in the observations between orbit directions were influenced by the diurnal cycle, therefore, obtaining the same correlations between directions indicates that the model performance is the same for any time of the day. Apparently, there are no times at which the model performs better than others.

Unfortunately there is no available collocated model data for the MetOps at 1-hourly sampling. Nevertheless, to analyse the effect of different collocated data sampling intervals, we have reprocessed the collocation model data for the HY-2B satellite at 3-hours interval as it is done with the MetOps so we can compare them in more similar conditions (Table 4.4).

Region	Resolution	Direction	MetOp-B 3-hourly	MetOp-C 3-hourly	**HY-2B 3-hourly**	HY-2B 1-hourly
North Atlantic	1/4º	ASC	0.18	0.15	**0.32**	0.51
		DES	0.16	0.17	**0.32**	0.46
Tropical Atlantic		ASC	0.04	0.04	**0.18**	0.30
		DES	0.03	0.03	**0.17**	0.29

Table 4.4: Comparison between the correlations between observations and collocated model data including a reprocessed 3-hourly NWP for HY-2B. The colour scheme and the rest of the values are the same as in table 4.3.

Table 4.4 demonstrates that the sampling interval of the collocated model data has a large impact on the correlation for the surface wind divergence. The HY-2B collocated with data sampled from the model at 3 hours intervals has significantly less correlation than the one from the same satellite with collocated data sampled at 1-hour intervals. Even so, the correlations for HY-2B with 3-hourly model data are still considerably higher than those from the MetOps in both regions. Therefore, the collocation sampling interval can only partially explain the differences between scatterometer instruments.

4.5 Spatial distribution of correlation between observations and their NWP collocated data

When talking about climatological data, there are a lot of details and conclusions that can not be obtained just by looking at data distribution without taking into account the spatial distributions of the values. In this section we will present the spatial distribution of the correlation found between the model and the observations. In the previous section we demonstrated the similarity of correlations for ascending and descending orbits and between satellites of the same family (ASCAT or HSCAT). Consequently, with the only goal of simplification in the visualisation, we will just present the plots for the satellites MetOp-B and HY-2B in descending orbit as representation of the ASCAT and HSCAT instruments respectively.

North Atlantic

Figure 4.8 presents the distribution of wind divergence observations, collocated data, the correlation between observations and collocated data for each gridpoint and the availability of values per gridpoint.

Regarding the wind divergence shown (positive values) and convergence (negative values) of the satellite observations (first column) over the North Atlantic, we can see the influence of the Gulf Stream in which it is possible to distinguish a strong surface convergence area probably driven by warm surface water and a surface divergence area in the vicinity of the convergence. The Gulf Stream is known to influence the surface divergence and convergence by its high amount of heat leading to convection and by the sea level pressure adjustments due to its SST pattern (Minobe et al. 2008).

When comparing the wind divergence perceived by the satellites and their collocated model data, we see a similar spatial pattern. That confirmed by mostly positive correlations between the observations and the model. In the case of HY-2B, the correlation is larger than for the MetOp-B. This is consistent with the results of the last section, a greater correlation for the HSCAT satellites. Some mechanisms that explain this higher correlation are the 1-hourly interval of collocated data from the model in the case of the Haiyang satellites in comparison with the 3-hourly collocated data of the MetOp satellites (Table4.4) and the lower variability of Haiyang observations and thus the less amount of extreme values (Section 4.1).

In addition, it is important to highlight that different patterns between the collocated model data for both satellites does not mean that the model is different, most of these differences are explained by the different time of the day of the satellite passes (at 9:30 and 21:30 for MetOp-B and at 6:00 and 18h for HY-2B) and by the difference in the sampling interval from the model to collocate the data (3-hourly for MetOp-B and 1-hourly for HY-2B).

Another notable difference are the data availability patterns (fourth column) for the HY-2B and MetOp-B. Overall there are more observations for the HY-2B satellite than for the MetOp-B because its wider swath. However, some areas of lower availability of values are found for HY-2B (see ITCZ area on the lower right plot on the Figure 4.8). These structures indicate rain because

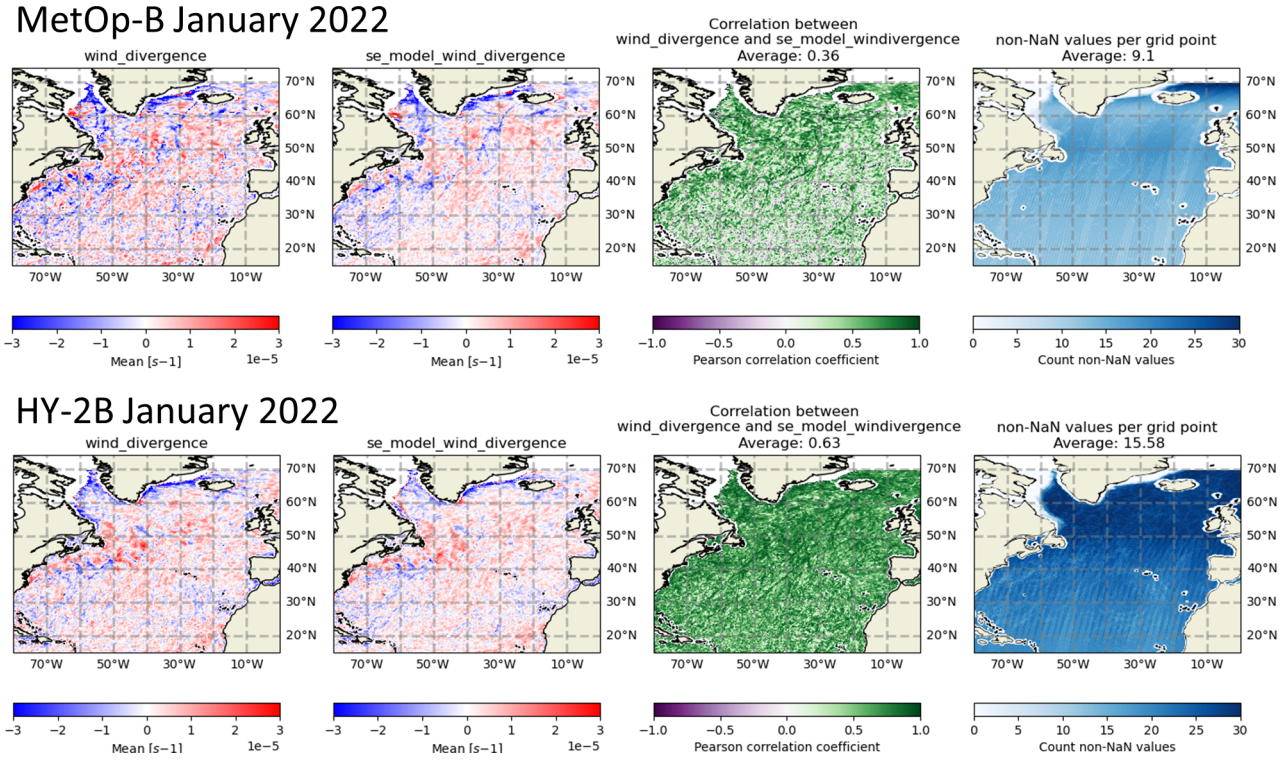

Figure 4.8: North Atlantic region. From left to right: Wind divergence observations, collocated wind divergence from NWP, Correlation between observations and collocated NWP and count of values available per gridpoint. Period January 2022 for MetOp-B (upper subplots) and HY-2B (lower subplots)..

for HSCAT satellites, the data is masked whenever it is raining due to the influence of rain drops in K_u-Band antennas.

Tropical Atlantic

Figure 4.9 shows the same analysis for the Tropical Atlantic region: distribution of wind divergence observations, collocated data from the model, correlation between observations and collocated model data and the amount of available values per gridpoint for the month of January 2022.

Observations of wind divergence and convergence over the Tropical Atlantic clearly show the influence of the ITCZ between the latitudes 0°-10°N (see first column of plots in the Figure 4.9). The ITCZ is characterised by permanent low pressure, convection and high amounts of precipitation which makes surface wind to converge at the surface level (Webster 2020). That is consistent with what the observations show.

The collocated model data, also shows the ITCZ but there are some important differences between the model and the observations for both satellites. First, the model does not present as much extreme values as the observations, especially for the MetOp-B observations. Second, observations from HY-2B and MetOp-B show a region with intense surface divergence (red) next to the ITCZ region (from the South) in the center of the Tropical Atlantic (around 0°N and between 10°W-25°W) which does not appear in the plots of collocated data from the model. Further analysis of the significance of these differences will be done in section 4.6. In addition, an underrepresentation of convergence over the ITCZ can be observed as it was also reported by Belmonte Rivas & Stoffelen (2019).

The correlation between observations and the collocated data from the model, is in the Tropical

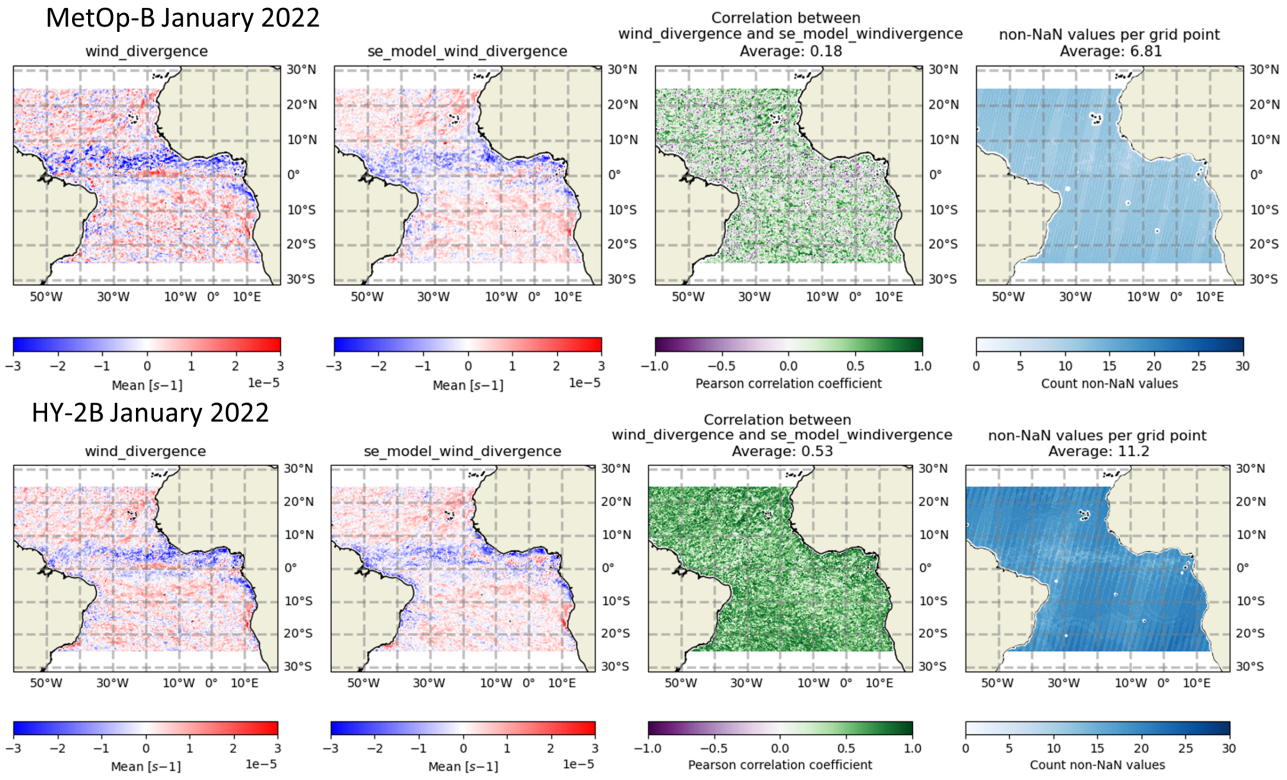

Figure 4.9: Tropical Atlantic region. From left to right: Wind divergence observations, collocated wind divergence from NWP, Correlation between observations and collocated NWP and count of values available per gridpoint. Period January 2022 for MetOp-B (upper subplots) and HY-2B (lower subplots).

Atlantic much lower than the one seen in the North Atlantic. This was already expected based on the results from the past sections . It is also consistent with what it was presented by Belmonte Rivas & Stoffelen (2019) who pointed out that ERA products have biases in the ITCZ . Therefore, more analysis will be done for the Tropical Atlantic region in order to see the evolution of these biases and their significance (Section 4.6).

The availability of observations (and therefore collocated data) for both satellites, is again greater for HY-2B because this satellite covers more world's surface in each orbit due to the wider swath. It is also noticeable how for the HY-2B there are less observations in the ITCZ region because of the higher number of precipitation events that occur there forcing data masking from any HSCAT instrument.

4.6 Tropical Atlantic 2022 evolution and significance of the biases

The spatial analyses of the correlation and comparison between observations and collocated data model in the Tropical Atlantic have shown that there are some big biases over the ITCZ. Nevertheless, those biases could be influenced by a low amount of observations or a big variability of the region which could make them less significant. To quantify this, a statistical hypothesis testing has been proposed.

Taking advantage of the east-west symmetry of the ITCZ, we can perform the analysis for the 2022 whole year in a Hovmöller diagram so that we present the results in a diagram of latitudes vs months. This is possible by averaging over longitudes and months. To do so, we combine both ASCAT satellites (MetOp-B and MetOp-C) for one of their orbit directions because they pass every

gridpoint more or less at the same local time, around 9:30 (Descending) and 21:30 (Ascending). The previous sections have shown how similar the data is from Metop-B and MetOp-C. We will be able to point the significance of the biases more accurately if we analyse the data from both satellites together.

Defining a significance of 99% ($\alpha = 0.01$) and computing a Statistical Hypothesis t-student Test whose null hypothesis (H_0) is that the mean of the observations is the same as the one of the collocated data from the model, we can affirm that the populations are significantly different if that null hypothesis is rejected (Equation 3.8).

ASCAT instruments (MetOp-B + MetOp-C Descending orbit)

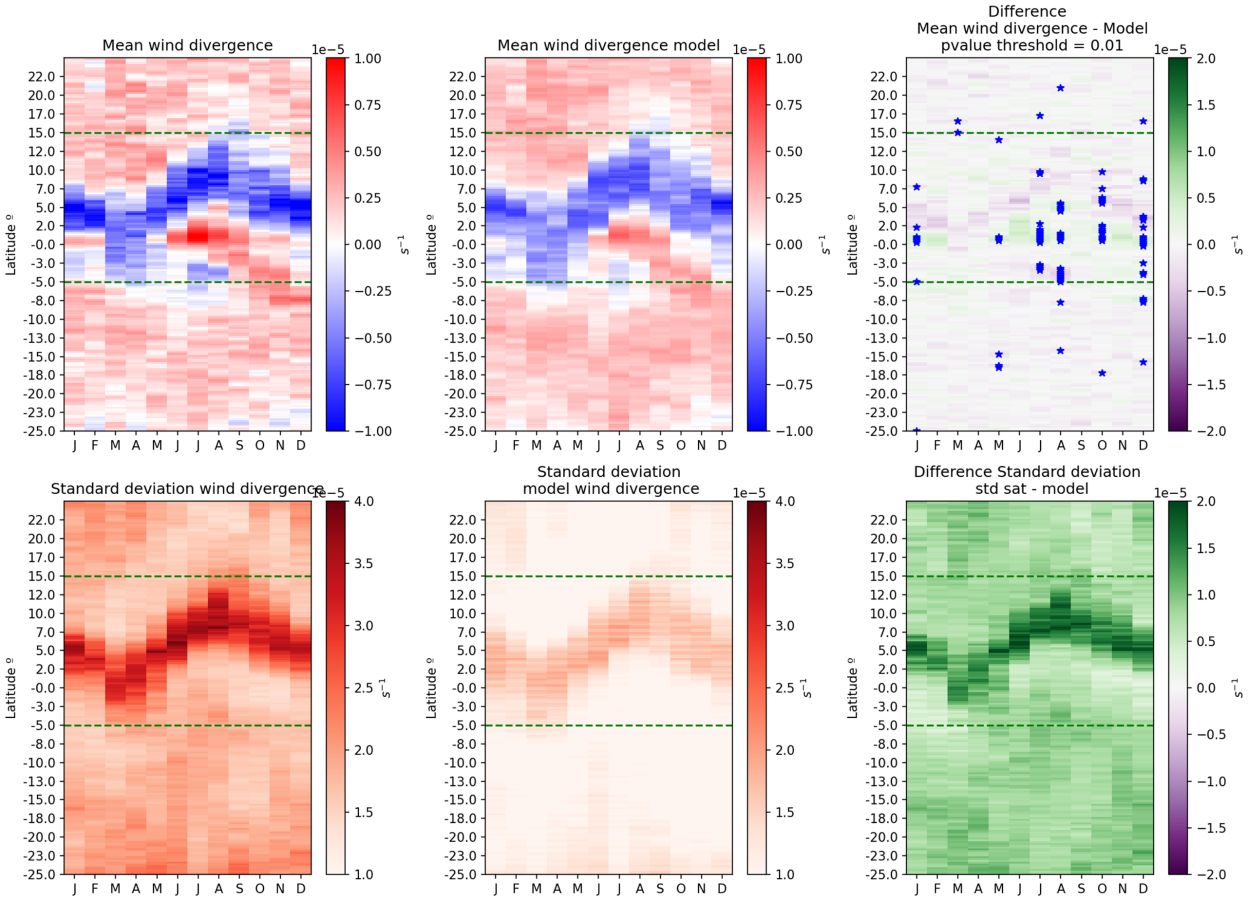

Figure 4.10: Hovmöller diagrams computed from MetOp-B and MetOp-C descending orbit data and its collocated NWP for the year 2022. Upper subplots correspond to observations (left), collocated model (middle) and difference between observations and model (right) for wind divergence. The same distribution of plots is used for the standard deviation of the wind divergence in the lower part of the figure. Blue stars indicate a significance of 99% or higher and the dashed green line designates the borders of the ITCZ.

Left subplots of Figure 4.10 show the seasonal evolution of the ITCZ for wind divergence from the ASCAT observations . The ITCZ shifts between 5°S and 15°N and is characterised by wind convergence (blue colour in the figure) over the surface for the whole year. It is important to highlight the wind divergence (red colour) that is found on the observations for the month of January around 0°N of latitude because the model was not able to forecast as divergence in this area. In addition, the lower subplots showing the wind divergence standard deviation, present the high variability of the ITCZ as it is expected because of the instability of the atmosphere there.

The comparison between the collocated model data Hovmöller and the observations, shows that although the model describes the same shift of the ITCZ as the observations, there are some significant differences between them. First, the standard deviation of the model is lower compared to the observations (Figure 4.10 lower right). This highlights again the lower variability of model shown in the earlier results. Second, when computing the difference between observations and collocated model data, there is an underrepresentation of the wind convergence over the ITCZ (colour purple on the top right subplot of Figure 4.10) which is consistent with the previous work of Belmonte Rivas & Stoffelen (2019). In addition, the model shows defective wind divergence south of the ITCZ for the whole year 2022.

The defective wind divergence south of the ITCZ was already localised in the spatial distribution (Figure 4.9). The Statistical Hypothesis Test marks it as a significant difference with a significance of more than 99% pointed by blue stars in the subplot. Overall there are other significant differences between observations and the collocated model data especially for wind divergence south of the ITCZ for the summer months and January, October and December 2022 (blue stars in Figure 4.10).

In the previous results it was seen that the Haiyang observations were closer to the collocated model data than the MetOp observations. There were still some differences, therefore, the same analysis is performed for the descending orbit of the HY-2B for the year 2022. In this case we cannot combine the observations with other satellites because we do not have data from HY-2C and HY-2D after March 2022. Even so, unlike the MetOps, those satellites pass at different times of the day, so it would not be as recommendable to merge the data between satellites.

HSCAT instrument (HY-2B Descending orbit)

HY-2B collocated model still show underrepresentation of wind convergence over the ITCZ compared to observations (Figure 4.11). However, the variability (standard deviation plots of Figure 4.11) is smaller compared to the MetOps (Figure 4.10). Consistently with the previous results, HSCAT instruments show less variability than ASCAT instruments but, in this case there is also some influence of the precipitation. The ITCZ is characterised as an area of high precipitation which is related with convection (wind convergence) and downbursts of wind (wind divergence). Whenever there is precipitation, the observations of HSCAT satellites are masked, as a result of that, some extreme values are not counted in the variability of the ITCZ.

The hypothesis test is also applied for the observations and collocations of HY-2B. There are less significant differences between observations and collocated model data for HY-2B than for the MetOps (Figure 4.10). Despite of that, January, July, August and December 2022 show significant differences. Therefore, the differences seen on the spatial distribution for January 2022 (Figure 4.9) have been proven to be significant from both scatterometer families ASCAT and HSCAT so the model is failing to represent the wind divergence south of the ITCZ around 0°N.

Similar results have been obtained for the ascending orbit direction for the MetOp and HY-2B satellites.

ASCAT spatial distribution of significant bias

The Hovmöller diagrams (Figure 4.10 and 4.11) present significant biases of the model in the Tropical Atlantic, especially south of the ITCZ. Observations from ASCAT and HSCAT agree on a stronger signal of positive wind divergence when comparing to model data. To locate where the stronger and more significant bias is coming from, the same statistical Hypothesis test (Section 3.2.6) is performed for every gridpoint of the Tropical Atlantic.

Figure 4.12 and 4.13 show that the majority of the significant bias is located in the positive wind divergence signal of the center of the Tropical Atlantic for January 2022. July 2022 also presents significant bias in the convergence of the Northwest coast of Brazil. These figures are also useful to show the seasonality of the ITCZ and its shifting between winter and summer. The same maps are computed for the HY-2B with a 3-hourly processing interval so it is the same as the

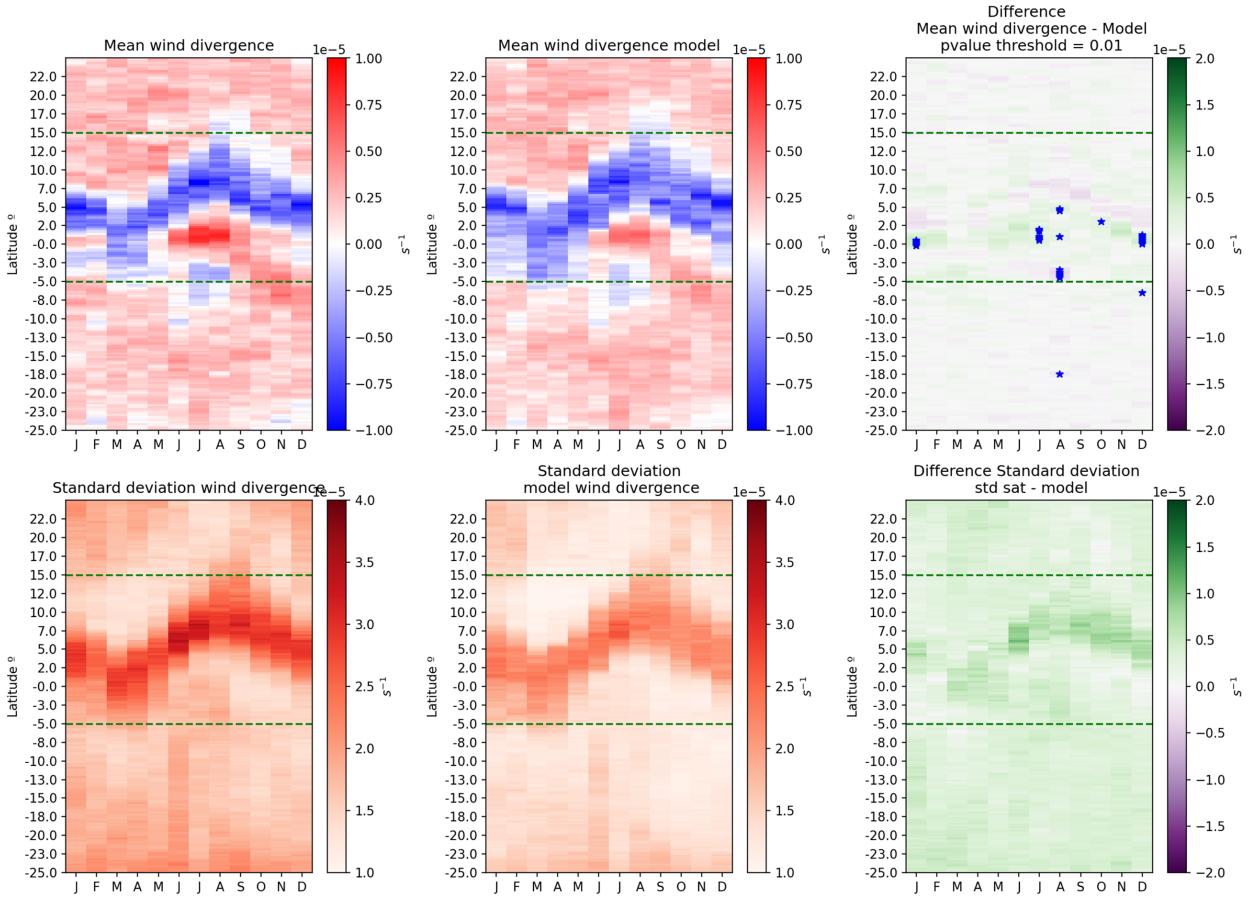

Figure 4.11: Hovmöller diagrams computed from HY-2B descending orbit data and its collocated NWP for the year 2022. Upper subplots correspond to observations (left), collocated model (middle) and difference between observations and model (right) for wind divergence. The same distribution of plots is used for the standard deviation of the wind divergence in the lower part of the figure. Blue stars indicate a significance of 99% or higher and the dashed green line designates the borders of the ITCZ.

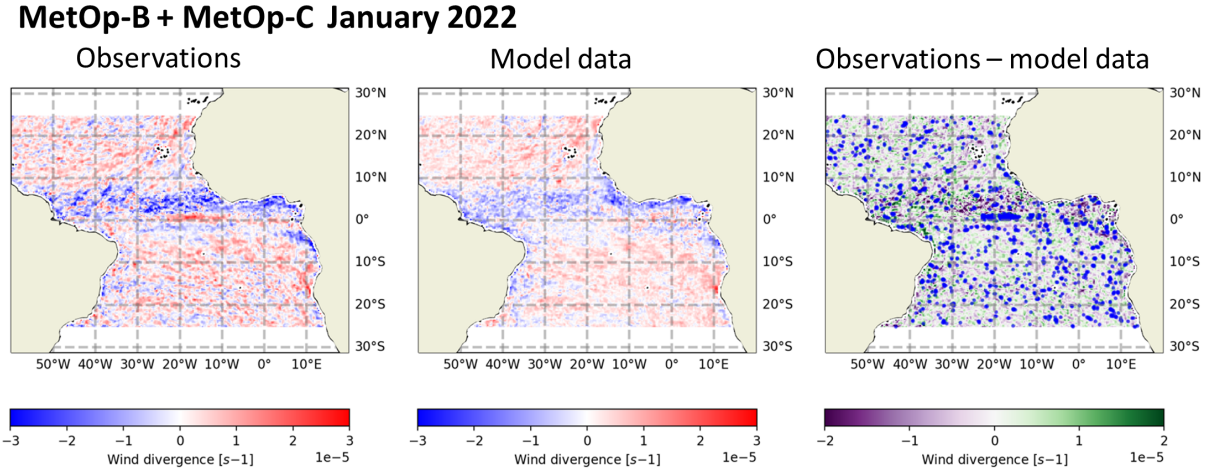

Figure 4.12: MetOp-B and MetOp-C descending orbits combined. Observations, collocated model and differences. Significant bias (pvalue ≤ 0.01) indicated with a blue dot. January 2022.

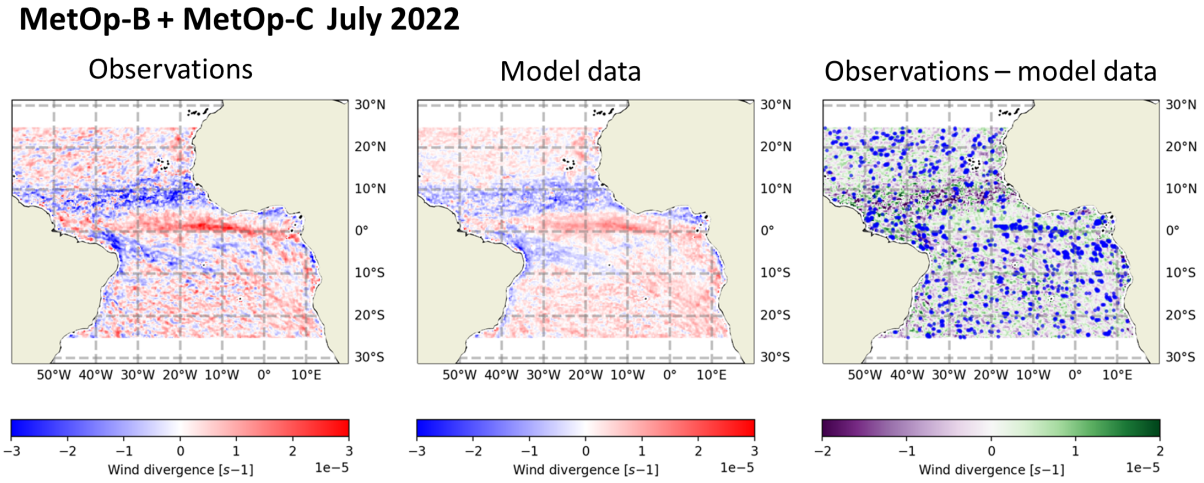

Figure 4.13: MetOp-B and MetOp-C descending orbits combined. Observations, collocated model and differences. Significant bias (pvalue ≤ 0.01) indicated with a blue dot. July 2022.

MetOps processing interval (Appendix A). As expected from the higher correlation and less bias of the model when compared to HSCAT observations, HY-2B presents less significant differences. Even so, they are located in the same areas.

4.7 Bias between observations and collocated NWP

In Section 4.4 the correlations between the observations and the NWP data were computed for the interval January-March 2022. In the sections 4.5 and 4.6 it was shown that there are some biases of the model in certain locations, especially over the ITCZ on the Tropical Atlantic. In this section, the biases will be copmuted for increasing intervals of the observed wind divergence to see if there is more bias between observations and collocated data for extreme values or not.

To perform that analysis, the difference between observations and the collocated model data has been computed so we have a value of the bias for each observation. Plotting these bias values as function of the observation values creates a cloud of points which is difficult to analyse. For simplification of the representation, it was decided to create 20 bins for each satellite to average the bias found in each of those intervals (Figure 4.14).

This kind of analysis was already used by Wang et al. (2020) to compute the biases of wind speed from ASCAT and HSCAT scatterometers with their collocated ERA5 wind speed data. The overall result from that analysis was that the more extreme the value of the observation was, greater the bias was found on average.

Figure 4.14 shows the average bias per observation for the 5 available satellites at $1/4^{o}$ resolution plus the two MetOps also at $1/8^{o}$ resolution. If there was no correlation between the model and the observations, a line following y = x would be expected and if the correlation was maximum, a horizontal line at y = 0 would appear.

North Atlantic bias

MetOp satellites biases over the North Atlantic, especially the high resolution ones ($1/8^{o}$) draw an almost straight line (Figure 4.14) which means that the bias is non dependent on the value of observation. The line that the biases for MetOp satellites on the North Atlantic describe is close to y = x but still between y = x and y = 0, therefore, the correlation is greater than 0. Comparing the biases between the ASCAT satellites and the HSCAT, it is seen how for any interval of values, there

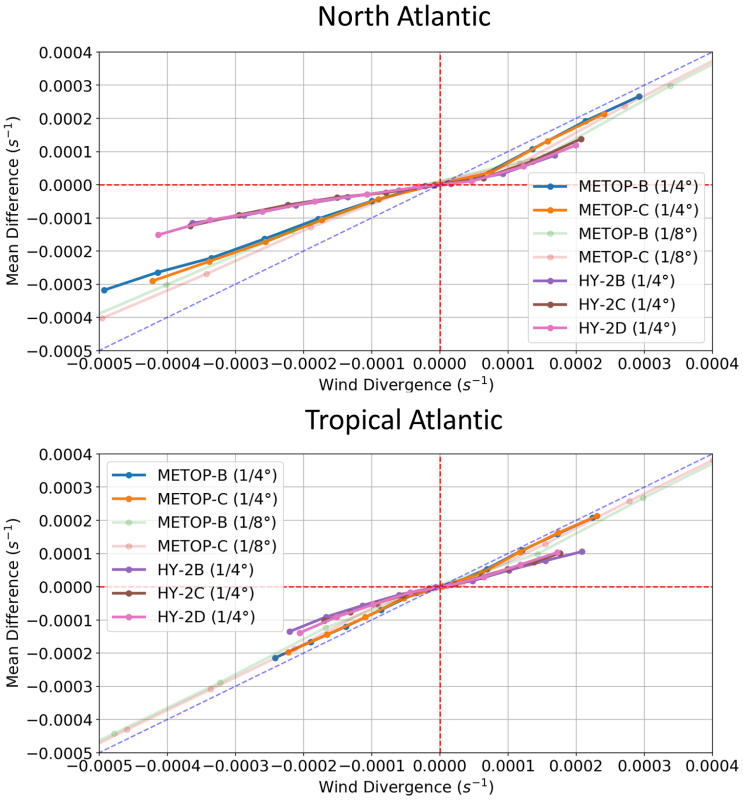

Figure 4.14: All available satellites at 1/4º plus the MetOp satellites also at 1/8º resolution averaged difference between observations and collocated data over observation values for the North Atlantic (left) and the Tropical Atlantic (right). Data from descending orbits in January-March 2022

is less bias for HSCAT satellites than for the ASCAT ones. Besides that, the HSCAT collocated data bias describe a curve suggesting that the more extreme observations have the greater the biases. This curve is very clear for the positive values of the observations (divergence) because for the first intervals it is almost horizontal and for greater values its slope increases until the bias almost coincides the y = x line.

In addition, a greater amount of extreme values for the MetOp satellites has been observed in comparison to the Haiyang ones, which is consistent with what has been found throughout this project. Besides that, slightly less bias is observed on the convergence side for the 1/4º resolution than for the 1/8º MetOps.

Tropical Atlantic bias

Similar results to the ones discussed for the North Atlantic have been obtained for the Tropical Atlantic. Again, less bias is found between collocated model data and HSCAT satellites than for the ASCAT satellites. Nevertheless, this time ASCAT satellites describe a straight line following y = x, which means that there is no correlation between the observations and the collocated data model, therefore, the bias is maximum.

In general, Tropical Atlantic biases are larger than the biases for the North Atlantic for all the satellites. This could be caused by the larger biases the model presents on the Tropical Atlantic or by a more variable physical phenomena over the Tropical Atlantic than over the North Atlantic. Collocated data is sampled at intervals of 1-hour or 3-hours, therefore, if that interval is larger than Tropical Atlantic phenomena time scales, the bias would be larger. Further analysis about the lifetime of the extreme values is presented in Section 4.8.

One of the reasons for the greater bias of ASCAT satellites in comparison with HSCAT satellites is the 3-hourly sampling intervals that the ASCAT use for the collocated data. To understand up to what extent this interval affects the bias, a comparison between MetOp-B (3-hourly interpolated) and HY-2B interpolated 1-hourly and 3-hourly is carried out (Figure 4.15).

Comparison between 1-hourly and 3-hourly collocations for HY-2B and 3-hourly MetOp-B

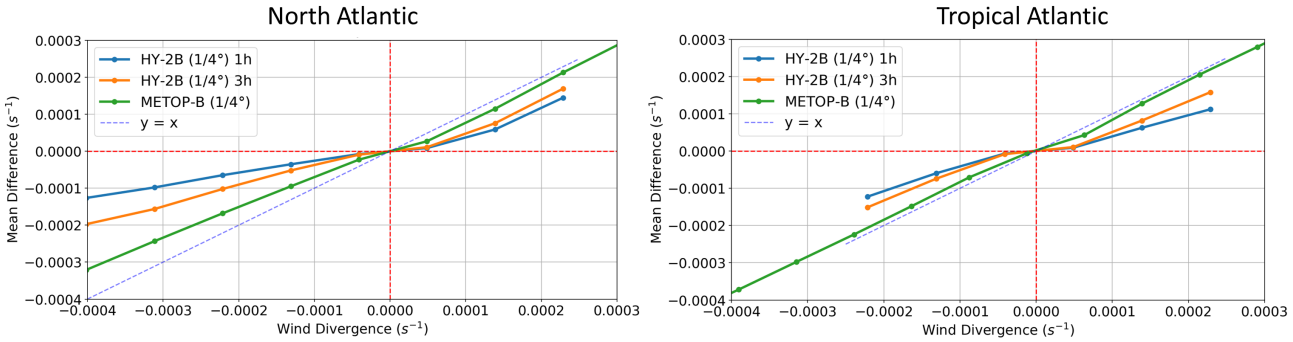

Figure 4.15: HY-2B 1-hourly and 3-hourly collocated data averaged difference between observations and collocated data over observation values for the North Atlantic (left) and the Tropical Atlantic (right). Data from descending orbits in January-March 2022

1-hourly HY-2B collocated data bias is clearly lower than 3-hourly for both regions. This is consistent with what the results from Section 4.4, where the correlation was higher for the 1-hourly interpolated HY-2B. In addition, it is visible that for low wind divergence, between $-1 \cdot 10^{-5} s^{-1}$ and $+1 \cdot 10^{-5} s^{-1}$ there is no significance difference between the 1-hourly and 3-hourly bias (for the HY-2B satellite). This suggests that phenomena of low intensity wind divergence is more stable than the extreme values of wind divergence.

Although the sampling rate from the model for the collocation data of the satellites influences the bias, the effect is not enough to explain the larger biases seen on the ASCAT satellites. Comparing to the values from of the biases from MetOp-B (which is collocated with 3-hourly sampled model data) to the biases of the 3-hourly HY-2B, we still find the bias from the HY-2B smaller than for the MetOp-B. Therefore, as in the correlation, the collocated data sampling interval is significant but it does not explain all the differences between the ASCAT and HSCAT instruments.

4.8 Analysis on wind divergence extremes based on ASCAT observations

A possible issue when comparing observations with the collocated model data is that the time scale of some of the physical phenomena involved is smaller than the time interval in which the NWP is sampled. Therefore, this section aims to understand the time scales of the extreme values. The reason behind this decision is that in the last section (4.7) the bias was observed to be maximum for the extreme values.

Following the 2σ criterion introduced in Section 3.2.3, and the advantage of MetOp-B and MetOp-C overlapping swaths, a computation of the proportion of extreme values that are observed in a time interval of 50 minutes will be conducted. This is only feasible using MetOp-B and MetOp-C satellites due to its specific orbits that make MetOp-C observations to be taken 50 minutes after MetOp-B or vice versa.

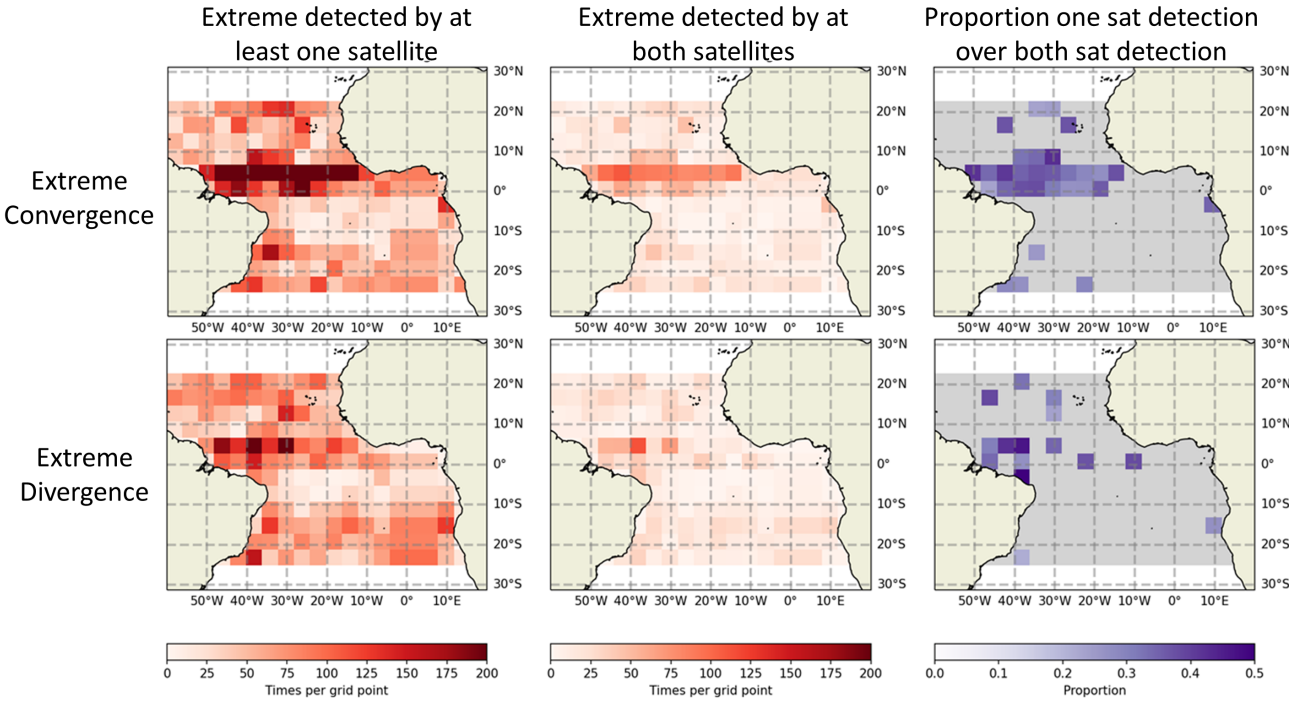

Figure 4.16: January 2022 extreme value analysis in the tropical Atlantic region per grid cell. Left column: frequency of extreme values observed by at least one satellite. Middle column: frequency of extreme values observed by both satellites. Right column: proportion of times both satellites detect an extreme compared to at least one satellite. Plots computed for extreme convergence (upper) and divergence (lower).

All the results are presented in groups of 256 gridpoints in grid cell of 4^{o} by $4^{o}$to be able to visualise the different behaviour of extremes depending on the region with a significant amount of values per gridpoint. As expected, the majority of extreme convergence values occur over the ITCZ region, between 0° and 10°N (Figure 4.16). In addition, in this region we also find the majority of values that are detected by both satellites which is influenced by the absolute amount of extreme convergence events.

In order to characterise the time scale of the extreme wind convergence and divergence, the proportion of occurrences when an extreme value is found by both MetOp satellites and a extreme value of the same sign is found by just one of the satellites is determined (rigth plots Figure 4.16). All the grid cells that did not reach at least 30 extreme observations for at least one satellite were masked to avoid non significant results.

As seen in Figure 4.16, the extreme convergence over the ITCZ region is detected by both satellites around 20%-40% of the times an extreme is found by one of the satellites. Besides that, some areas of the ITCZ also present extremes of surface wind divergence but those phenomena are restricted to the western part of the equatorial Atlantic. Observing both types of extremes in the same grid cells of the ITCZ illustrate the great variability that is observed in this area as it was seen in the previous results.

Some grid cells were masked due to the lack of data, as a result of limiting the analysis to just January 2022. Therefore, the ratio of both satellites observing an extreme value and at least one satellite observing the same kind of extreme has been computed for the whole 2022 (Figure 4.17). The same proportion is computed for the North Atlantic. In the case of the North Atlantic, due to the change from ascending to descending orbit, the results are only be analysed up until latitude 50^{o}N because for farther north latitudes the observations should also include the opposite orbit

direction of the satellite.

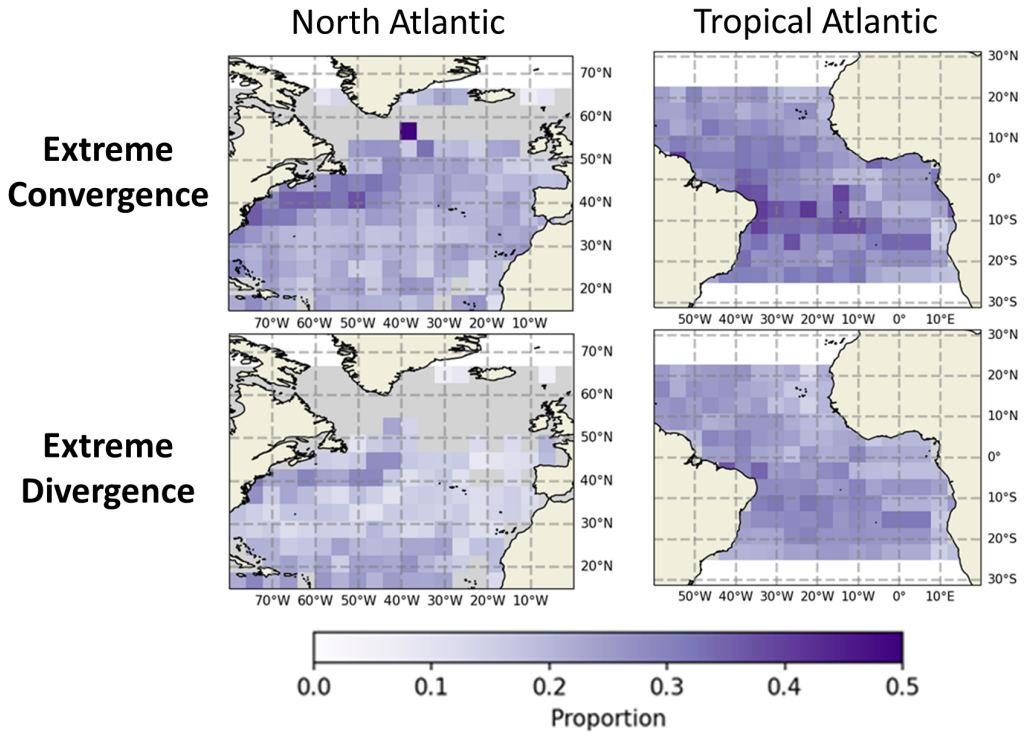

Figure 4.17: 2022 extreme value analysis in the North Atlantic (left) and Tropical Atlantic (right) per grid cell. Proportion of times both satellites detect an extreme compared to at least one satellite. Plots computed for extreme convergence (upper) and divergence (lower) from 1/4º resolution MetOp-B and MetOp-C descending orbits

Although the largest amount of extreme convergence values observed by both satellites were found over the ITCZ, the fraction of extreme convergence is greater south of the ITCZ than over it. This suggests that south of the ITCZ the mechanisms that generate extreme convergence have longer time scales so both satellites capture the extremes.

The influence of Gulf Stream and it characteristic extreme convergence values in the North Atlantic is clearly visible. The proportion of extreme convergence values found per extreme value observation is significantly higher than in the rest of the North Atlantic, being 40% of the times for the Gulf Stream region vs 20% of the times for the rest of the North Atlantic. The high SST of the Gulf Stream creates wind surface convergence as it was already explained by Minobe et al. (2008).

Figure 4.17 shows clear differences between regions and between extremes of convergence and divergence. In both regions, the proportion of extremes for wind convergence is higher than for extreme wind divergence. This indicates a higher prevalence in time of extreme convergence for each gridpoint than extreme divergence which leads to the conclusion that processes that generate extreme convergence have a longer lifetime than the ones that generate extreme wind divergence. For example, a process that creates extreme wind divergence is the wind downbursts of intense precipitation which usually has a very short time scale (King et al. 2022), therefore, it makes sense that in 50 minutes the value of wind divergence is not extreme anymore.

The comparison between wind convergence and divergence extremes shows that in a general aspect, after 50 minutes the same extreme value can be seen in 20% to 40% of the times, being 40% for the Gulf Stream and western Equatorial Atlantic extreme surface wind convergence and 20% or less for the rest of the areas, especially in the case of extreme wind divergence. However,

the values that are not considered extremes, in other words, every value between -2σ and +2σ, has not been analysed yet. Therefore, to understand how much these values change in a time lapse of 50 minutes, a 2D density map and a regression has been computed for the entire spectrum of wind divergence observations between Metop-B and MetOp-C (Figure 4.18). In the case of the North Atlantic region, the northern boundary has been reduced to 50ºN so the results are consistent with the analysis of Figure 4.17.

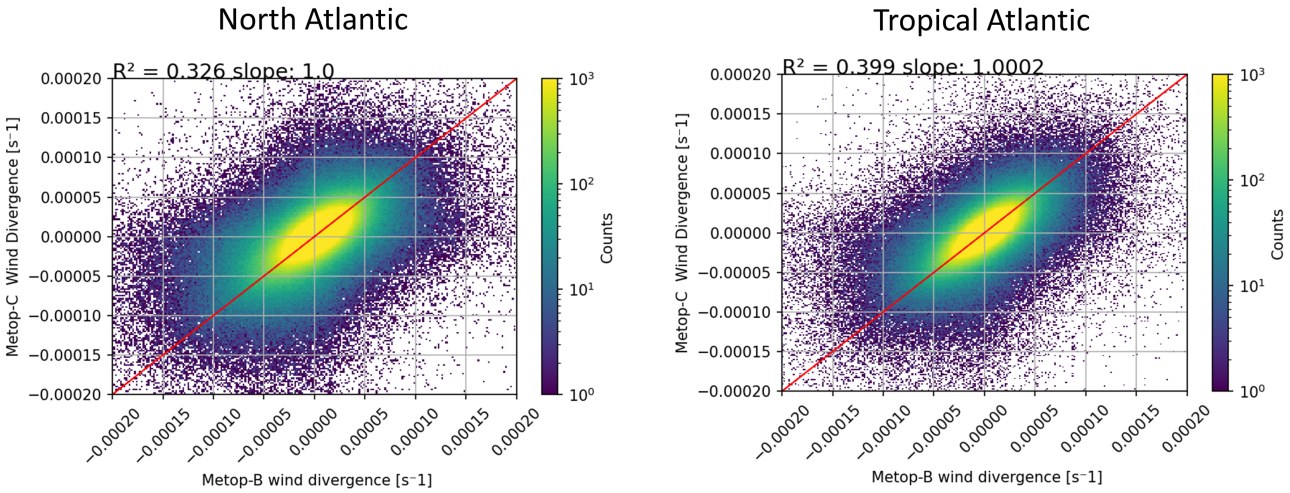

Figure 4.18: 2D density plots of overlapping 1/4° MetOp-B and MetOp-C wind divergence observations for North Atlantic (left) and Tropical Atlantic (right) regions. Linear regression line is plotted in red.

The 2D density plots for the North Atlantic and the Tropical Atlantic regions show a positive correlation between MetOp-B and MetOp-C for both regions (Figure 4.18). The squared Pearson correlation coefficient for the North Atlantic is $R^2 = 0.326$, while for the Tropical Atlantic, it is $R^2 = 0.399$. This difference is already visible in the 2D density plot when comparing the two regions. In the North Atlantic, the values are more dispersed in every direction compared to the Tropical Atlantic region. In addition, by looking at the way the values are distributed in the 2D density plots, it can be seen that there are slightly more extreme values of convergence than divergence, especially on the North Atlantic. It is also interesting to visualise that the slope of the linear regression is 1 for both regions, that back ups the idea of both ASCAT satellites to have the same data distribution as it was seen in previous results.

4.9 Differences between 1/8º and 1/4º resolution from ASCAT instruments

One of the results provided by the analysis of data distribution and its evolution (Sections 4.1 and 4.3) is the high standard deviation, low skewness and low kurtosis that the high resolution datasets have in comparison with the ones of lower resolution. For this reason, in this section we will make a comparison between the 1/4° (25 km) and 1/8° (12.5 km) MetOps data distribution and their statistical parameters.

At Level 1 Metop-B at 1/4° resolution and at 1/8° resolution have a different spatial processing, a hamming filter is used for the 1/8° dataset and a top hat filter is used for the 1/4° resolution dataset (Section 3.1.1). Therefore a smoother value is expected from the 1/4° resolution dataset than from the 1/8°. To understand better what the differences are between the 1/8° and 1/4° resolution MetOps, a smoothing from the 1/8° to 1/4° is performed in a manner where the averaged

values are matching the original 1/4° grid.

The 1/8° and 1/4° grids at Level 3 are created in such a way that the gridpoints of the 1/4° one are located in between each 4 points of the 1/8° grid, precisely in the middle of the square that those 4 gridpoints describe. Therefore, the smoothing process makes groups of 4 points (2 by 2 in a square) and the averaged values is calculated. Since the 1/4° grid is exactly in the middle of these squares, the average is not weighted. All the original four 1/8° values used were located at the same distance from the new gridpoints.

The new averaged dataset from 1/8° to 1/4°, from now on called "averaged 1/4°", is compared with the original 1/8° and the original 1/4° in the spatial distribution so we can understand better what the role of the distribution for the surface wind divergence.

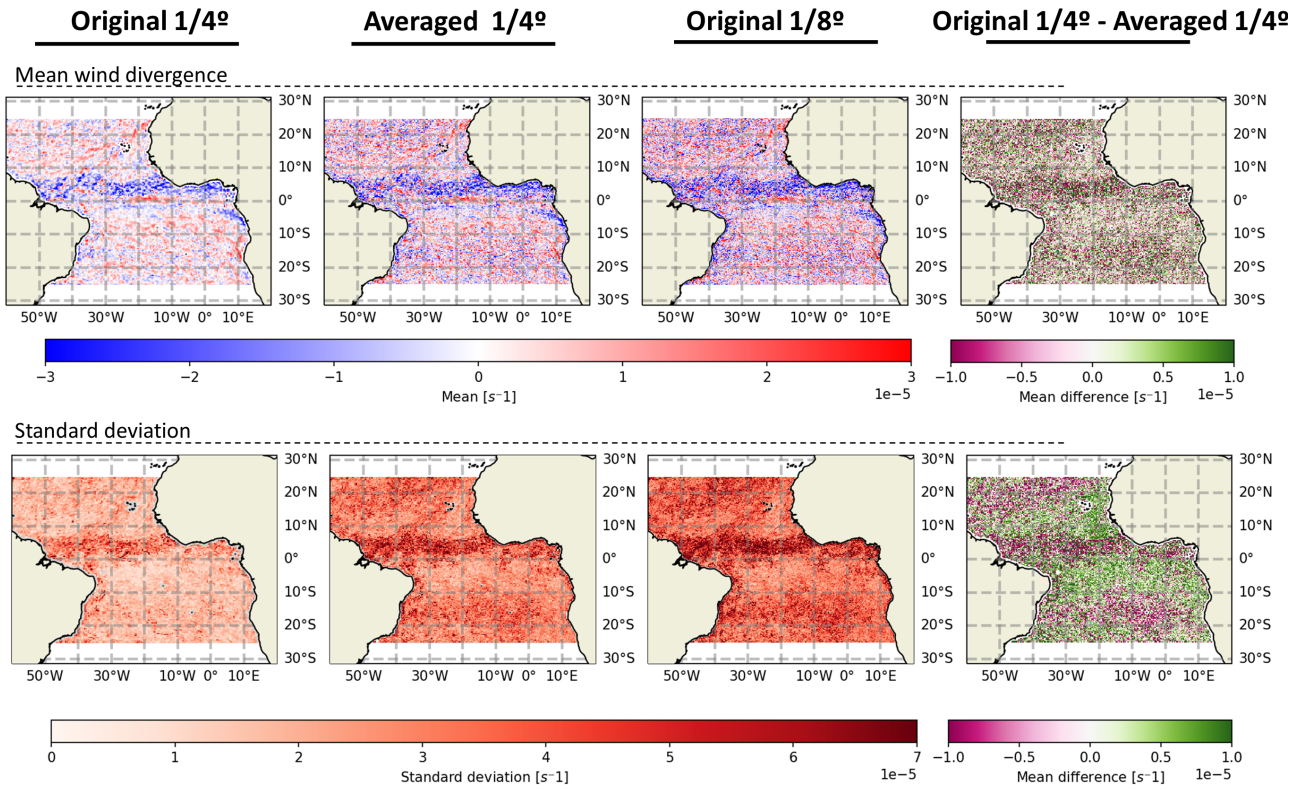

Figure 4.19: From left to right in columns: Original 1/4°, averaged 1/4°, original 1/8° and the difference between the original 1/4° and the averaged one. Means have been substracted for the differences. In the upper part the mean wind divergence is presented and in the lower part the standard deviation. All the data used is from descending orbits of MetOp-B of January 2022.

Figure 4.19 shows mean wind divergence and standard deviation over the Tropical Atlantic for the original 1/4°, the averaged 1/4°, the original 1/8° and the difference between the original 1/4° and the averaged 1/4°. To compute this last difference, the mean has been subtracted so it is easier to appreciate the differences in the small scale.

Comparing the two original resolutions, a smoother signal is found in the 1/4° original resolution, while in the 1/8° one, more extreme values are present. Section 4.1 is consistent with this finding because 1/8° MetOps observations were presenting more extreme values than 1/4° observations. The standard deviation is also consistent with the data distribution. 1/8° resolution observations have on average a higher standard deviation.

Regarding the mean wind divergence spatial distribution from Figure 4.19, the expectation is that smoothing over the 4 nearest neighbours would give a similar distribution as the original 1/4°.

Nevertheless, the averaged 1/4° spatial distribution still shows more small scale extremes of wind divergence than the original 1/4°. In addition, looking at the statistical parameters for the three different configurations (original 1/4°, averaged 1/4° and original 1/8°) the values of the averaged 1/4° and the original 1/8° are closer to the normal distribution (Table 4.5).

North Atlantic	**1/4° Original**	**1/4° Averaged**	**1/8° Original**
Std (s^{-1})	2.82E-05	5.09E-05	4.26E-05
Skewness	-2.03	-1.02	-0.78
Kurtosis	28.57	17.83	9.10

Tropical Atlantic	**1/4° Original**	**1/4° Averaged**	**1/8° Original**
Std (s^{-1})	2.32E-05	4.77E-05	3.83E-05
Skewness	-0.92	-0.40	-0.20
Kurtosis	17.47	16.33	8.41

Table 4.5: Statistical parameters for comparison between original 1/4° and 1/8° resolutions and averaged 1/4° resolution. Data computed from year 2022 for North Atlantic (left) and Tropical Atlantic (right) from descending orbits of MetOp-B

As seen in the Figure 4.19, the standard deviation values of the averaged 1/4° dataset is less than the ones of the original 1/8° because of the spatial smoothing but it is still larger than the original 1/4°. The same applies to the North Atlantic, also with the skewness and kurtosis. Taking into account that the wind divergence for the original 1/4° resolution was computed as the spatial derivatives of its 4 nearest neighbours at Level 2 and that the same was done at Level 3 for the smoothing of the 1/8° to 1/4°, we can say that there are some small scale influences in the data of the original 1/8° that are still influential when it is averaged to 1/4°.

The previously commented spatial averaging done at Level 1 is consistent with the obtained results. Even after matching the resolutions, the datasets in which the smoother spatial filter was applied (Hamming filter to 1/4° dataset) presents smoother values than the one with the sharper filter (Top Hat filter applied to 1/8° dataset). Another explanation would be a normally distributed noise propagated in the processing of the high resolution MetOps data that makes its statistical parameters to be closer to the normal distribution. In addition, that would explain why the correlation between 1/8º MetOps and the collocated model data is in the order of 0.01 (Table 4.3).

4.10 Analysis of the diurnal cycle from non Sun-synchronous satellites

Up until now, we have mainly used the satellites MetOp-B, MetOp-C and HY-2B due to their more data availability of data over 2022 and because of their Sun-Synchronous orbits. With this kind of orbit the observations are collected at the same local time everyday and therefore, the diurnal cycle isolated from from the observations. Nevertheless, the non-Sun-synchronus orbits of the HY-2C and HY-2D can be used for the study of the diurnal cycle because the observations are taken at a different local time every day.

Figure 4.20 shows the difference in intervals between the wind divergence of every observation (from HY-2C and HY-2D) and the averaged wind divergence of the entire January 2022 so it is possible to see the areas that change in function of what time of the day it is. In addition, since the Tropical Atlantic covers a wide range of longitudes. The UTC time is converted to the local time so the time intervals displayed are the local solar time (LST). Compared to the North Atlantic, diurnal cycle in the Tropical Atlantic is larger due to the greater variation in the solar radiation over the day, therefore, that is the region analysed.

The main result is the strong signal of sea breeze cycle along the coasts of Africa. For the intervals 00h-06h and 06h-12h, the wind divergence difference with the daily average in the coastal water is negative, which indicates that there is convergence over the ocean. On the other hand, the

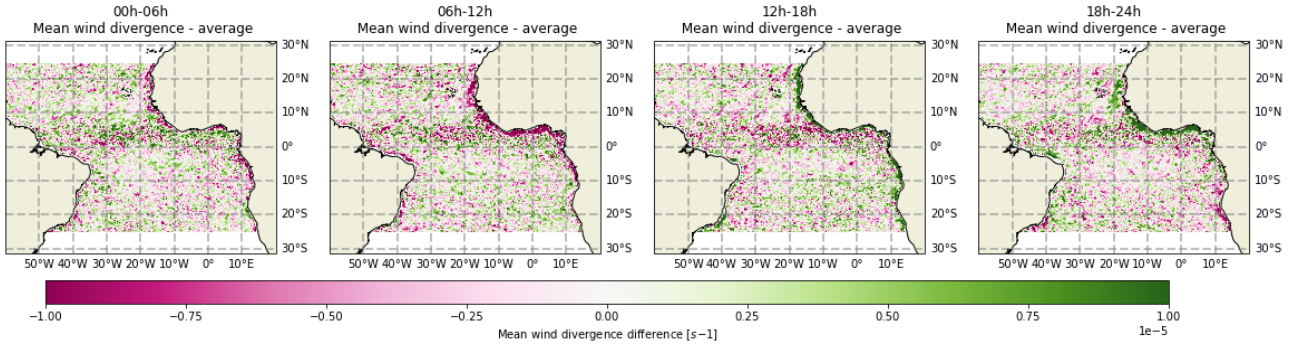

Figure 4.20: Differences between averaged wind divergence within given intervals (00h-06h, 06h-12h, 12h-18h, 18h-24h) and the averaged 1-day wind divergence from ascending and descending observations of HY-2C and HY-2D. Data of January 2022 for the Tropical Atlantic region.

intervals 12h-18h and 18h-24h, show a positive signal of wind divergence difference with the daily average day. Which is the result of wind divergence over the ocean. These results are consistent with a local higher pressure over the cold side in the pair land-ocean and a local low pressure on the warm side. A low pressure will make winds to converge and the opposite happens with the high pressure (Dai & Deser 1999). Therefore, we find winds from high to low pressure which means that surface winds blow from land to ocean during the night (the ocean is warmer) and from the ocean to the land during the day, when the land is warmer.

Chapter 5

Conclusion and discussion

This MSc thesis has studied surface wind divergence properties and the differences between this wind divergence and the collocated operational ECMWF model. All of this has been possible due to level 3 processed data of the satellites MetOp-B, MetOp-C, HY-2B HY-2C and HY-2D. Limitations, conclusions and possible future work on this field will be discussed in this section.

5.1 Limitations

This study is conducted with data available for the year 2022, therefore, no climatological analysis can be done. Even so, seasonal patterns that match the expected climatology have been found. Besides that, for the non-Sun-Synchronous satellites, processed data was available from January to March 2022 so for those satellites there is no possibility to compute the 2022 evolution.

Regarding the geophysical representation of the wind, it is based on the wind stress-equivalent winds because those are the winds that scatterometers can measure. Therefore, all the results are based on those winds and not on the real winds. In any case, this does not affect the comparison with the operation ECMWF model because the data has been converted from neutral winds to stress equivalent winds.

Furthermore, data collocation from the model to the satellite is influenced by its spatially and temporally averaging which may modify the model data distribution. The ECMWF operational model output used has a resolution of 9 km and the resolution that is mainly used throughout this project is 1/4° (25 km), the spatial collocation method averages it with the 4 nearest points weighted as $1/r^2$. The higher spatial resolution of the model in comparison with the observations, and taking into account how the observations are smoothed (Section 3.1.1), does not make the collocated values to be significantly smoother. On the other hand, the temporal smoothing done during the collocation is computed as a linear interpolation between the two closest forecasts of the model which are available each 3 hours for the MetOps and 1-hour for the Haiyangs. This averaging smooths the values of the collocated data, therefore when comparing observations and collocated model data some part of the higher dispersion found on the observations is explained by this averaging. Sections 4.4 and 4.7 show the effect of how the collocation model intervals affect the correlation and bias between collocated model values and observations.

Last, processing of 1/4° MetOps at Level 1 is not the same as the processing of the MetOps at 1/8° and the HY satellites as it is explained in Section 3.1.1 because of the filtering algorithms that are used. In addition, in Section 4.9 it was seen that different processing mechanisms may impact the statistical parameters and the spatial distribution of the data. Therefore, when comparing 1/4° MetOps data to the rest of the satellites we should take into account that the data processing was

different.

These limitations make it harder to draw conclusions from the obtained results. Nevertheless, after considering the limitations, some conclusions can be stated.

5.2 Conclusions

Comparison between collocated ECMWF model and observations

This study focuses on the comparison between surface wind divergence observations from scatterometers and their collocated model data in space and time. Multiple ways of analysing the differences between them have been explored throughout of this thesis. It is clear that the results are influenced by numerous factors as resolution, instrument, orbit direction, etc. However, a consistent finding is that there is less correlation and more difference between collocated data and observations in the Tropical Atlantic than in the North Atlantic, which could indicate that the model biases are higher in that region. Another explanation for this phenomenon could be higher temporal variability in the Tropical Atlantic. As a result of that, the 1-hourly and 3-hourly sampling intervals would be too long to explain the phenomena in this region.

In order to understand and characterise the temporal scale of wind divergence phenomena in each region, the 50-minute offset and overlap of orbits provided by MetOps satellites were used (Section 4.8). The results obtained, show that the North Atlantic experiences greater variations in wind divergence values within a 50-minute interval compared to the Tropical Atlantic. The findings imply that the greater disparity between observations and the model in the Tropical Atlantic, in contrast to the North Atlantic, can be attributed to a higher bias in the model specifically for the Tropical Atlantic region. This observation is consistent with previous publications as Belmonte Rivas & Stoffelen (2019).

Regardless of the temporal averaging applied, it still makes sense to compare observations with the model. For example, for the area south of the ITCZ in January 2022, the sign of the wind divergence bias is opposite for scatterometer and collocated model data (Section 4.6). Even taking into account that the collocated data is averaged, a change on the sign of the wind divergence cannot be explain by that averaging.

Therefore, as an overall main conclusion on the differences between scatterometer observations and the ECMWF operational model, we could say that more bias is found on the Tropical Atlantic than in the North Atlantic for the year 2022. In addition, this bias is proved to be significant for some areas of the ITCZ region with two satellites with very different technologies: ASCAT and HSCAT.

Comparison between different scatterometers

Consistent with what it was expected from previous studies on scatterometers wind data (Wang et al. 2020), ASCAT instruments from MetOp-B and MetOp-C report a very similar data distribution when compared in the same resolution (Section 4.1). In addition, HSCAT satellites (HY-2B, HY-2C and HY-2D) also present a similar data distribution between them, although, unlike HY-2C and HY-2D, HY-2B has a sun-synchronous orbit. In the comparison between ASCAT and HSCAT instruments, it can be seen that the ASCAT satellites present more variability, more skewness towards convergence data and more proportion of extremes when compared to the HSCAT ones. Moreover, when compared to model data, HSCAT satellites are closer than ASCAT ones. This can be explained by the smaller proportion of extreme values that HSCATs observe, probably due to

the different technology of the antenna and data retrieving. The smother values presented by the Haiyangs result in closer correspondence to the model.

Therefore, looking at model biases, MetOp satellites will display larger biases. It may sound counterintuitive that the satellites that are less correlated with the model are better to test the model because we may think that they are less accurate. Nevertheless, scatterometers product evaluation articles e.g. Wang et al. (2020), demonstrate that ASCAT satellite observations are more reliable than HSCAT. They have a higher ratio of successful observations (mainly because they do not interfere with rain) and their biases in wind speed are in the order 0.01 m/s in comparison with the 0.1 m/s found for HY-2B using the same validation method based on buoy winds.

Other conclusions

First, MetOp-B and MetOp-C allowed us to study the time scale of extreme divergence over the North Atlantic and Tropical Atlantic (Section 4.8), finding that extreme convergence phenomena have larger time scales than extreme divergence. An explanation for this finding is that extreme divergence is often linked with very intense rain and its downbursts of wind, which often does not last the 50 minutes that it takes the MetOps to scan the same area. On the other hand, extremes of surface wind divergence are related with deep convection and cloud formation which can last for more than 50 minutes. This idea is supported by the spatial distribution of extremes observed by the MetOps, being the Tropical Atlantic and the Gulf Stream region the more prone areas for deep convection.

Second, It is notable the ability of non-Sun-Synchronous satellites to describe the diurnal cycle as it shown with HY-2C and HY-2D.

Last, through a bias analysis (Section 4.7), it has been shown that the differences in the accessing intervals between MetOps and Haiyangs (1-hour and 3-hour intervals) do not explain all the differences between the biases encountered by the satellites.

5.3 Possible future work

Based on the results, limitations and conclusions obtained along this project, some recommendations for future work can be stated.

The whole project is based on the year 2022, therefore, it does not allow for the analysis of longer timescales than a year. It would be interesting to extend the observation period of to multiple years to study the effects of phenomena that occur over longer timescales such as ENSO. To illustrate this, one of the results obtained was that January, July, August and December of 2022 had a significant model bias. It would be very interesting to study whether the model is more likely to be biased in these seasons or if this was just the case in the year 2022. Nevertheless, extending the period of analysis would not be possible for many years because the lifetime of the satellites is limited and a lot of them were launch very recently. To illustrate this, MetOp-C, HY-2B, HY-2C and HY-2D were launched in 2018 or later (Table 1.1). However if those satellites keep working as planned, we will have a period of overlapping observations for more than five years.

In addition, the comparison between MetOps data at 1/8° resolution and 1/4° resolution was not able to clarify the differences between the resolutions because the spatial processing of the data was different. It is recommended to work with the same type of processing for every resolution so they can be compared in more detail. A new study on the role of the resolutions is proposed for data processed in the same way.

Furthermore, the interpolation in time from the model output to the collocated data smooths over wind divergence values making conclusions harder to get when comparing with direct scat-

terometer observations. It is suggested a new version of collocated data with the values of the closest model output without any kind of interpolation so the data does not get averaged in time. Having both types of collocations would help on the analysis of the differences between observations and model data.

All the collocated data for this project comes from the same configuration of the same operational model. A study of the biases of different models or different versions of the same model may provide a better understanding of the model biases.

Furthermore, it has been shown how 1-hourly intervals of accessing model output reduce the difference between the observations and the collocated data. However, MetOps and Haiyangs datasets did not have the same intervals. It is suggested to collocated model data for MetOps also in 1-hourly intervals so they match the intervals of the Haiyang collocated values.

Last, this project has been restricted to the North Atlantic and Tropical Atlantic, hence, it is proposed to extend the analysis to other areas and understand where the differences are coming from. Belmonte Rivas & Stoffelen (2019) already studied biases of ERA5 and ERA-Interim in comparison with ASCAT observations from MetOp-A on a global scale. Their analysis could be extended with the satellites used for this project and the ECMWF operational model used for the collocations.

Appendix A

HY-2B Spatial significant bias

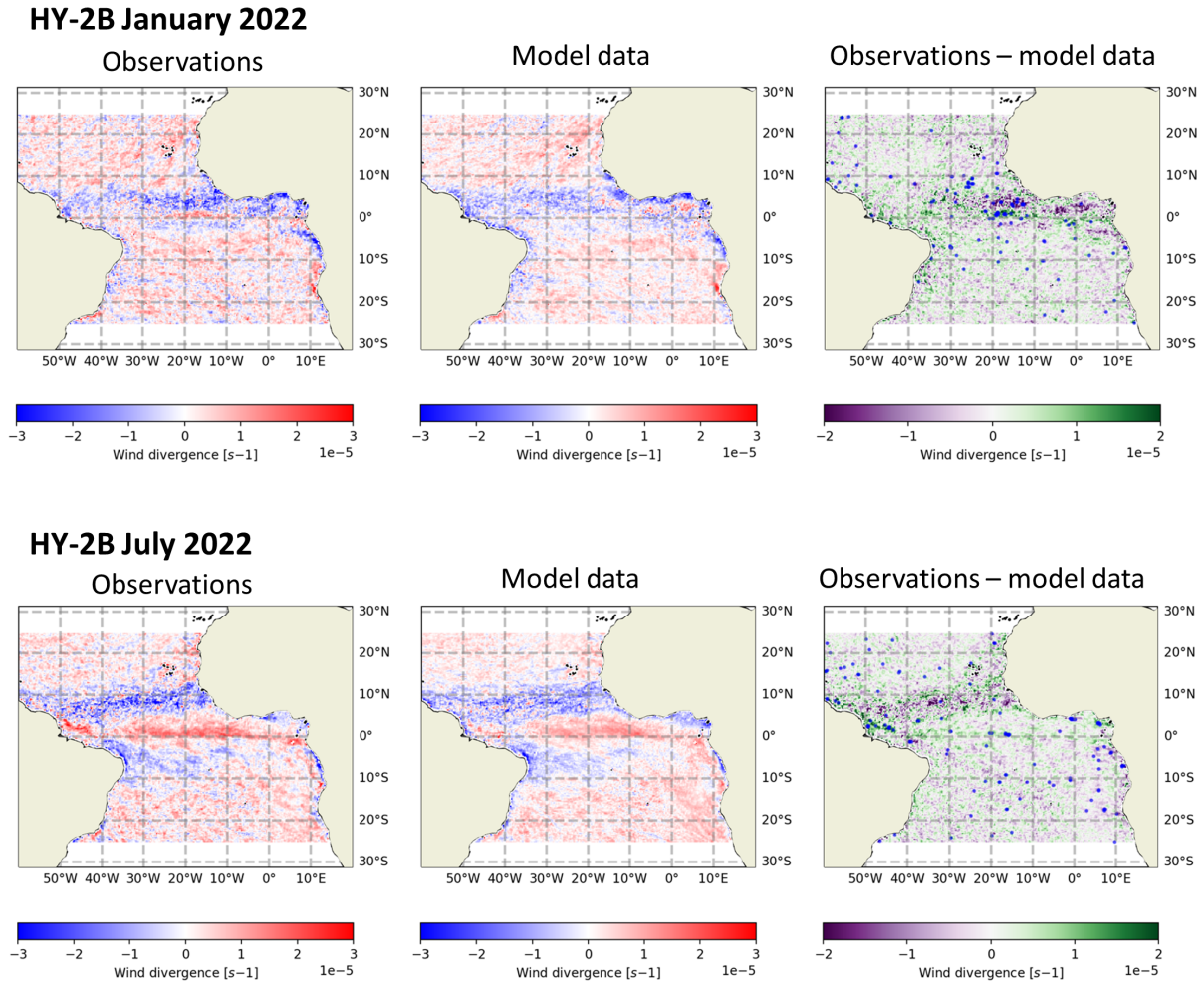

Figure A.1: 3-hourly processed HY-2B descending orbit data. Observations, collocated model and differences. Significant bias (pvalue ≤ 0.01) is indicated with a blue dot. Time frame January and July 2022.

To use the same intervals of model output access, the same maps as Figure 4.12 has been calculated for HY-2B with its data collocation accessed 3-hourly to match it with the accessing intervals of the MetOps. Significant biases are found on the same location as the ones found by the MetOps but with less significant gridpoints.

Bibliography

Atlas, R., Hoffman, R. N., Ardizzone, J., Leidner, S. M., Jusem, J. C., Smith, D. K. & Gombos, D. (2011), 'A cross-calibrated, multiplatform ocean surface wind velocity product for meteorological and oceanographic applications', *Bulletin of the American Meteorological Society* **92**(2), 157–174.

Belmonte Rivas, M. & Stoffelen, A. (2019), 'Characterizing ERA-Interim and ERA5 surface wind biases using ASCAT', *Ocean Science* **15**(3), 831–852.

Cronin, M. F., Gentemann, C. L., Edson, J., Ueki, I., Bourassa, M., Brown, S., Clayson, C. A., Fairall, C. W., Farrar, J. T., Gille, S. T. et al. (2019), 'Air-sea fluxes with a focus on heat and momentum', *Frontiers in Marine Science* **6**, 430.

Dai, A. & Deser, C. (1999), 'Diurnal and semidiurnal variations in global surface wind and divergence fields', *Journal of Geophysical Research: Atmospheres* **104**(D24), 31109–31125.

de Kloe, J., Stoffelen, A. & Verhoef, A. (2017), 'Improved use of scatterometer measurements by using stress-equivalent reference winds', *IEEE Journal of Selected Topics in Applied Earth Observations and Remote Sensing* **10**(5), 2340–2347.

ECMWF, I. (2021), 'Integrated Forecasting System'.
URL: *https://www.ecmwf.int/en/forecasts/documentation-and-support/changes-ecmwf-model*

ESA (2020), 'ESA - types of orbits'.
URL: *https://www.esa.int/Enabling_Support/Space_Transportation/Types_of_orbits*

EUMeTrain (2017), 'Tutorial on satellite derived wind products'.
URL: *https://resources.eumetrain.org/data/4/438/navmenu.php?tab=2&page=3.0.0*

Eumetsat (2021), 'HY-2B and HY-2C winds and services from the OSI SAF'.
URL: *https://osi-saf.eumetsat.int/community/stories/hy-2b-and-hy-2c-winds-and-services-osi-saf*

European Space Agency (2012).
URL: *https://www.eoportal.org/satellite-missions/metop*

Holton, J. R. (1973), 'An introduction to dynamic meteorology', *American Journal of Physics* **41**(5), 752–754.

Jones, W. L. (2015), Early days of microwave scatterometry: RADSCAT to SASS, *in* '2015 IEEE International Geoscience and Remote Sensing Symposium (IGARSS)', IEEE, pp. 4208–4211.

King, G. P., Portabella, M., Lin, W. & Stoffelen, A. (2022), 'Correlating extremes in wind divergence with extremes in rain over the Tropical Atlantic', *Remote Sensing* **14**(5), 1147.

Meyer, R. (2016), 'ASCAT Level 1: Product generation specification'.

Minobe, S., Kuwano-Yoshida, A., Komori, N., Xie, S.-P. & Small, R. J. (2008), 'Influence of the Gulf Stream on the troposphere', *Nature* **452**(7184), 206–209.

NASA (2021), 'Data processing levels'.
URL: *https://www.earthdata.nasa.gov/engage/open-data-services-and-software/data-information-policy/data-levels*

Nekrasov, A., Khachaturian, A., Abramov, E., Markelov, O. & Bogachev, M. (2019), 'On sea ice measurement by a C-band scatterometer at VV polarization: Methodology optimization based on computer simulations', *Remote Sensing* **11**(21), 2518.

NSOAS (2023).
URL: *http://www.nsoas.org.cn/eng/*

OSI SAF, E. W. (2019), 'ASCAT wind product user manual', *Version* **1**, 23.

OSI SAF Winds, T. (2021), 'Product User Manual (PUM) for the HY-2 winds: version 1.0', *Darmstadt: EUMETSAT* .

Pipis, G. (2020), 'Skewness and kurtosis in statistics'.
URL: *https://www.r-bloggers.com/2020/11/skewness-and-kurtosis-in-statistics/*

Stoffelen, A. (1998), 'Scatterometry', *PhD Thesis* .

Stoffelen, A., Verspeek, J. A., Vogelzang, J. & Verhoef, A. (2017), 'The CMOD7 geophysical model function for ASCAT and ERS wind retrievals', *IEEE Journal of Selected Topics in Applied Earth Observations and Remote Sensing* **10**(5), 2123–2134.

Stull, R. B. (2015), *Practical meteorology: an algebra-based survey of atmospheric science*, University of British Columbia.

Takatama, K., Minobe, S., Inatsu, M. & Small, R. J. (2012), 'Diagnostics for near-surface wind convergence/divergence response to the gulf stream in a regional atmospheric model', *Atmospheric Science Letters* **13**(1), 16–21.

Uppala, S. M., Kållberg, P., Simmons, A. J., Andrae, U., Bechtold, V. D. C., Fiorino, M., Gibson, J., Haseler, J., Hernandez, A., Kelly, G. et al. (2005), 'The ERA-40 re-analysis', *Quarterly Journal of the Royal Meteorological Society: A journal of the atmospheric sciences, applied meteorology and physical oceanography* **131**(612), 2961–3012.

Vogelzang, J. & Stoffelen, A. (2012), 'Scatterometer wind vector products for application in meteorology and oceanography', *Journal of Sea Research* **74**, 16–25.

von Schuckmann, K., Le Traon, P.-Y., Smith, N., Pascual, A., Djavidnia, S., Gattuso, J.-P., Grégoire, M., Aaboe, S., Alari, V., Alexander, B. E. et al. (2021), 'Copernicus marine service ocean state report, issue 5', *Journal of Operational Oceanography* **14**(sup1), 1–185.

Waliser, D. & Jiang, X. (2015), 'Tropical meteorology and climate— intertropical convergence zone'.

Wang, Z., Stoffelen, A., Fois, F., Verhoef, A., Zhao, C., Lin, M. & Chen, G. (2017), 'SST dependence of Ku-and C-band backscatter measurements', *IEEE Journal of Selected Topics in Applied Earth Observations and Remote Sensing* **10**(5), 2135–2146.

Wang, Z., Stoffelen, A., Zou, J., Lin, W., Verhoef, A., Zhang, Y., He, Y. & Lin, M. (2020), 'Validation of new sea surface wind products from scatterometers onboard the HY-2B and MetOp-C satellites', *IEEE Transactions on Geoscience and Remote Sensing* **58**(6), 4387–4394.

Wang, Z., Zou, J., Stoffelen, A., Lin, W., Verhoef, A., Li, X., He, Y., Zhang, Y. & Lin, M. (2021), 'Scatterometer sea surface wind product validation for HY-2c', *IEEE Journal of Selected Topics in Applied Earth Observations and Remote Sensing* **14**, 6156–6164.

Webster, P. J. (2020), *Dynamics of the tropical atmosphere and oceans*, John Wiley & Sons.

Wentz, F. J. & Smith, D. K. (1999), 'A model function for the ocean-normalized radar cross section at 14 GHz derived from NSCAT observations', *Journal of Geophysical Research: Oceans* **104**(C5), 11499–11514.

Zhang, Y., Mu, B., Lin, M. & Song, Q. (2020), 'An evaluation of the Chinese HY-2B satellite's microwave scatterometer instrument', *IEEE Transactions on Geoscience and Remote Sensing* **59**(6), 4513–4521.